ELSEVIER

Comput. Methods Appl. Mech. Engrg. 184 (2000) 213–239

Computer methods in applied mechanics and engineering

www.elsevier.com/locate/cma

Two-level domain decomposition methods with Lagrange multipliers for the fast iterative solution of acoustic scattering problems

Charbel Farhat [a,*], Antonini Macedo [a], Michel Lesoinne [a], Francois-Xavier Roux [b], Frédéric Magoulès [b], Armel de La Bourdonnaie [c]

[a] *Department of Aerospace Engineering Sciences and Center for Aerospace Structures, University of Colorado at Boulder, Boulder, CO 80309-0429, USA*

[b] *ONERA, Direction de l'Informatique, 29 Av. de la Division Leclerc, BP72 92322 Chatillon Cedex, France*

[c] *CERMICS/CAIMAN, INRIA BP.93 - F06902, Sophia Antipolis Cedex, France*

Abstract

We present two different but related Lagrange multiplier based domain decomposition (DD) methods for solving iteratively large-scale systems of equations arising from the finite element discretization of high-frequency exterior Helmholtz problems. The proposed methods are essentially two distinct extensions of the regularized finite element tearing and interconnecting (FETI) method to indefinite or complex problems. The first method employs a single Lagrange multiplier field to glue the local solutions at the subdomain interface boundaries. The second method employs two Lagrange multiplier fields for that purpose. The key ingredients of both of these FETI methods are the regularization of each subdomain matrix by a complex lumped mass matrix defined on the subdomain interface boundary, and the preconditioning of the global interface problem by a coarse second-level problem constructed with planar waves. We show numerically that both methods are scalable with respect to the mesh size, the subdomain size, and the wavenumber, but that the FETI method with a single Lagrange multiplier field – labeled FETI-H (H for Helmholtz) in this paper – delivers superior computational performances. We apply the FETI-H method to the parallel solution on a 24-processor Origin 2000 of an acoustic scattering problem with a submarine shaped obstacle, and report performance results that highlight the unique efficiency of this DD method for the solution of high frequency acoustic scattering problems.

MSC: 57; 49; 18; 20

1. Introduction

The d-dimensional scattering of time-harmonic acoustic waves by an impenetrable obstacle embedded in a homogeneous medium $\Omega \subset \mathbb{R}^d$ can be formulated as the following exterior Helmholtz boundary value problem

$$\begin{aligned} &-\nabla^2 u - k^2 u = f \quad \text{in } \Omega, \\ &u = g_1 \quad \text{on } \Gamma_{\mathrm{D}}, \\ &\nabla u \cdot v = g_2 \quad \text{on } \Gamma_{\mathrm{N}}, \\ &\lim_{r\to\infty} r^{(d-1)/2}\left(\frac{\partial u}{\partial r} - \mathrm{i}ku\right) = 0, \end{aligned} \tag{1}$$

* Corresponding author. Tel.: +1-303-492-3992; fax: +1-303-492-4990.
E-mail address: charbel@alexandra.colorado.edu (C. Farhat).

0045-7825/00/$ - see front matter
PII: S0045-7825(99)00229-7

where k is the wavenumber associated with the problem, f the prescribed forcing function, g_1 the prescribed Dirichlet data on the boundary Γ_D, g_2 the prescribed Neumann data on boundary Γ_N, and v is the unit outward normal on the boundary Γ_N. The last of Eq. (1) is the Sommerfeld radiation condition which ensures that all waves at infinity are outgoing.

The finite element discretization of the above boundary value problem leads to the following system of complex equations

$$\widetilde{\mathbf{K}}\mathbf{u} = \mathbf{f}, \quad \text{where } \widetilde{\mathbf{K}} = \mathbf{K} - k^2\mathbf{M} + \mathrm{i}k\mathbf{M}_S. \tag{2}$$

Matrices $\mathbf{K}$ and $\mathbf{M}$ are the so-called stiffness and mass matrices of the problem, and $\mathbf{f}$ its right-hand side vector. Matrix $\mathbf{M}_S$ is induced by the Sommerfeld radiation condition and is non-zero only at the degrees of freedom lying on the outer boundary of the computational domain. In the absence of of the Sommerfeld condition – that is, for the interior Helmholtz problem – $\widetilde{\mathbf{K}} = \mathbf{K} - k^2\mathbf{M}$ is usually an indefinite matrix. In this sense, $\widetilde{\mathbf{K}} = \mathbf{K} - k^2\mathbf{M} + \mathrm{i}k\mathbf{M}_S$ is also often called an indefinite matrix.

High-frequency acoustic scattering problems call for fine meshes, and therefore lead to large-scale systems of equations. For such problems, solving Eq. (2) by a direct method entails memory and CPU requirements that rapidly overwhelm even the largest resources that are currently available. For this reason, a significant amount of research continues to be invested in the development of Krylov-subspace, multigrid, and domain decomposition (DD) based iterative algorithms for the solution of the matrix problem (2) [1–7]. However, for high frequencies and therefore large values of the wavenumber k, $\widetilde{\mathbf{K}}$ is usually indefinite, which poses serious challenges to the analysis, implementation, and performance of iterative solvers.

In this paper, we present two scalable DD methods with Lagrange multipliers for the solution of exterior Helmholtz problems, and show that one of them is an amazingly powerful iterative solver for high-frequency acoustic scattering problems. The first DD method employs one Lagrange multiplier field and was first introduced in [8] as the FETI-H method. It is described in more detail in Section 2, which also introduces a novel coarse problem for the Helmholtz equation based on a two-level methodology and planar waves. The second DD method, which is based on the preliminary work described in [5], employs two Lagrange multiplier fields and is presented in detail in Section 3 of this paper. Both DD methods are essentially extensions to indefinite or complex problems of the regularized version [9] of the finite element tearing and interconnecting (FETI) method [10–13]. Here, we show that they are scalable with respect to the mesh size, the subdomain size, and the wavenumber. In Section 4, we discuss the relative merits of the FETI-H method and its two-field alternative. In Section 5, we apply the FETI-H method to the parallel solution of a two-dimensional acoustic scattering problem with a submarine shaped obstacle. We report impressive performance results on a 24-processor Origin 2000 that highlight the efficiency of the FETI-H method for the solution of high frequency acoustic scattering problems. Finally, we conclude this paper in Section 6.

2. Domain decomposition with one Lagrange multiplier field

2.1. A modified Lagrangian formulation

For the sake of clarity, we consider first the case where $\mathbf{M}_S = 0$ (the interior Helmholtz problem), and Ω is partitioned into two non-overlapping subdomains Ω^1 and Ω^2. In Section 2.3, we generalize the DD method proposed herein to the exterior Helmholtz problem and the case of arbitrary mesh decompositions. Note that by Ω we mean the mesh associated with the given domain, and therefore it is the mesh that is partitioned into subdomains. Hence, in this paper we consider only subdomains with matching interfaces.

Let $\mathbf{K}^s$, $\mathbf{M}^s$, $\widetilde{\mathbf{K}}^s = \mathbf{K}^s - k^2\mathbf{M}^s$, and $\mathbf{f}^s$ denote respectively the stiffness matrix, mass matrix, problem matrix, and right-hand side vector associated with subdomain Ω^s, $s = 1, 2$, and let $\mathbf{u}^s$ denote the restriction to Ω^s of the solution of problem (2). For each subdomain, we also introduce a *signed* Boolean matrix $\mathbf{B}^s$ that extracts from a given subdomain vector a signed interface boundary component. The sign of that component is specified by the orientation of the normal to the corresponding subdomain interface. For example, using

this notation, the continuity of the subdomain solutions across the subdomain interfaces can be written as $\sum_{s=1}^{s=N_s} \mathbf{B}^s\mathbf{u}^s = 0$. Furthermore, we partition $\mathbf{u}^s$ into two components

$$\mathbf{u}^s = \begin{bmatrix} \mathbf{u}_i^s \\ \mathbf{u}_b^s \end{bmatrix}, \tag{3}$$

where the subscripts i and b designate internal and interface boundary unknowns, respectively.

Given an interface matrix $\mathbf{S}_{bb}$ – that is, a matrix defined on the interface between subdomains Ω^1 and Ω^2 – we construct the following modified Lagrangian [9]

$$\begin{aligned} \mathscr{L}(\mathbf{v}^1, \mathbf{v}^2, \lambda) &= \frac{1}{2}\mathbf{v}^{1^{\mathrm{T}}}\tilde{\mathbf{K}}^1\mathbf{v}^1 - \mathbf{f}^{1^{\mathrm{T}}}\mathbf{v}^1 + \frac{1}{2}\mathbf{v}^{2^{\mathrm{T}}}\tilde{\mathbf{K}}^2\mathbf{v}^2 - \mathbf{f}^{2^{\mathrm{T}}}\mathbf{v}^2 + \boldsymbol{\lambda}^{\mathrm{T}}(\mathbf{B}^1\mathbf{v}^1 + \mathbf{B}^2\mathbf{v}^2) + \frac{1}{2}\left(\mathbf{v}_b^{1^{\mathrm{T}}}\mathbf{S}_{bb}\mathbf{v}_b^1 - \mathbf{v}_b^{2^{\mathrm{T}}}\mathbf{S}_{bb}\mathbf{v}_b^2\right) \\ &= L(\mathbf{v}^1, \mathbf{v}^2, \lambda) + \frac{1}{2}\left(\mathbf{v}_b^{1^{\mathrm{T}}}\mathbf{S}_{bb}\mathbf{v}_b^1 - \mathbf{v}_b^{2^{\mathrm{T}}}\mathbf{S}_{bb}\mathbf{v}_b^2\right), \end{aligned} \tag{4}$$

where $\boldsymbol{\lambda}$ is a vector of discrete Lagrange multipliers defined on the interface between Ω^1 and Ω^2, and the superscript T designates the transpose of a quantity.

Solving problem (2) is equivalent to finding the stationary points $\mathbf{u}^1$ and $\mathbf{u}^2$ of the modified Lagrangian $\mathscr{L}$. Indeed, $L(\mathbf{v}^1, \mathbf{v}^2, \boldsymbol{\lambda})$ is the classical Lagrangian function of a two-subdomain problem, and the quantity $\frac{1}{2}(\mathbf{v}_b^{1^{\mathrm{T}}}\mathbf{S}_{bb}\mathbf{v}_b^1 - \mathbf{v}_b^{2^{\mathrm{T}}}\mathbf{S}_{bb}\mathbf{v}_b^2)$ depends only on the traces of $\mathbf{v}^1$ and $\mathbf{v}^2$ on the interface between Ω^1 and Ω^2. Since the vector of Lagrange multipliers λ enforces the continuity equation $\mathbf{B}^1\mathbf{v}^1 + \mathrm{B}^2\mathbf{v}^2 = 0$ on the interface between Ω^1 and Ω^2, it follows that the stationary points $\mathbf{u}^1$ and $\mathbf{u}^2$ of $\mathscr{L}$ are independent of the choice of the interface matrix $\mathbf{S}_{bb}$. Let $\mathbf{S}_I^s$ denote the subdomain matrix defined as zero inside Ω^s and as $\mathbf{S}_{bb}$ on the interface boundary between Ω^1 and Ω^2. Using the same partitioning as in Eq. (3), $\mathbf{S}_I^s$ can be written as

$$\mathbf{S}_I^s = \begin{bmatrix} 0 & 0 \\ 0 & \mathbf{S}_{bb} \end{bmatrix}, \quad s = 1, 2. \tag{5}$$

The Euler equations associated with the modified Lagrangian $\mathscr{L}$ are then given by

$$\begin{aligned} &(\tilde{\mathbf{K}}^1 + \mathbf{S}_I^1)\mathbf{u}^1 = (\mathbf{K}^1 - k^2\mathbf{f}^1 + \mathbf{S}_I^1)\mathbf{u}^1 = \mathbf{f}^1 - \mathbf{B}^{1^{\mathrm{T}}}\boldsymbol{\lambda}, \\ &(\tilde{\mathbf{K}}^2 - \mathbf{S}_I^2)\mathbf{u}^2 = (\mathbf{K}^2 - k^2\mathbf{f}^2 - \mathbf{S}_I^2)\mathbf{u}^2 = \mathbf{f}^2 - \mathbf{B}^{2^{\mathrm{T}}}\boldsymbol{\lambda}, \\ &\mathbf{B}^1\mathbf{u}^1 + \mathbf{B}^2\mathbf{u}^2 = 0. \end{aligned} \tag{6}$$

The role of the interface matrix $\mathbf{S}_{bb}$ is now clear. For a given discretization of both subdomains Ω^1 and Ω^2, the prescribed wavenumber k may correspond to a resonant frequency of Ω^1 and/or Ω^2. In other words, k^2 may coalesce with an eigenvalue of either or both pencils $(\mathbf{K}^1, \mathbf{M}^1)$ and $(\mathbf{K}^2, \mathbf{M}^2)$. In such a case, either or both local problems described in Eq. (6) become ill-posed when $\mathbf{S}_{bb} = 0$. Hence, the purpose of a carefully constructed $\mathbf{S}_{bb}$ is to prevent the singularity of the subdomain matrix problems. We note that this issue has already been addressed in the literature, albeit with a different perspective (for example, see [1,3]).

However, we would like to emphasize that as far as the design of a DD based iterative solver is concerned, it is not the potential singularity of a subdomain matrix problem that is problematic as much as the characterization of this singularity. For example, if both subdomain Helmholtz problems are ill-posed ($\mathbf{S}_{bb} = 0$), the solution of Eq. (6) can be written as

$$\begin{aligned} \mathbf{u}^1 &= \tilde{\mathbf{K}}^{1^+}\left(\mathbf{f}^1 - \mathbf{B}^{1^{\mathrm{T}}}\boldsymbol{\lambda}\right) + \tilde{\mathbf{N}}^1\boldsymbol{\alpha}^1, \\ \mathbf{u}^2 &= \tilde{\mathbf{K}}^{2^+}\left(\mathbf{f}^2 - \mathbf{B}^{2^{\mathrm{T}}}\boldsymbol{\lambda}\right) + \tilde{\mathbf{N}}^2\boldsymbol{\alpha}^2, \end{aligned} \tag{7}$$

where $\tilde{\mathbf{K}}^{s^+}$ is a generalized inverse of $\tilde{\mathbf{K}}^s$, and the columns of $\tilde{\mathbf{N}}^s$ generate a basis of the null space of $\tilde{\mathbf{K}}^s$. For elasticity problems ($k = 0$) where the subdomain matrix problems can also be singular, it was shown in [10–13] that if the dimension of ker $(\mathbf{K}^s)$ and the columns of the corresponding matrix $\mathbf{N}^s$ can be easily determined, the ill-posed nature of the subdomain problems can be exploited to construct an auxiliary coarse problem for the target DD method that propagates the error globally, accelerates convergence, and ensures scalability with respect to the subdomain size H. In other words, ill-posed subdomain problems are not always detrimental to the formulation of a DD method.

For elasticity problems, except in some pathological cases, the exact dimension of the null space of the stiffness matrix of a floating subdomain can be easily determined, as it is independent of the mesh size h [14]. A generalized inverse of that stiffness matrix can also be rapidly computed during its factorization [14]. Here, by floating subdomain we mean a subdomain without sufficient essential boundary conditions to prevent its stiffness matrix $\mathbf{K}^s$ from being singular. Unfortunately, the same cannot be said for Helmholtz problems. Indeed, given a discretization for a subdomain, it is practically impossible to determine whether k^2 is a true eigenvalue of the pencil $(\mathbf{K}^s, \mathbf{M}^s)$, or whether it is numerically "close" to an eigenvalue of that pencil. It is not easy either to determine the multiplicity of that eigenvalue. And most importantly, whether k^2 coalesces or not with an eigenvalue of the pencil $(\mathbf{K}^s, \mathbf{M}^s)$ depends on the size of the mesh h, which complicates further the issues. For all these reasons, it is preferable for Helmholtz problems to regularize the subdomain matrices $\mathbf{K}^s$ with an interface matrix $\mathbf{S}_{bb}$ as proposed once in the regularized FETI method [9], rather than attempt to compute a general form of the subdomain solutions as described in Eq. (7). It remains to address the issue of how to construct a regularizing interface matrix $\mathbf{S}_{bb}$.

One way to avoid local resonance is to introduce local damping, which suggests that $\mathbf{S}_{bb}$ should be a complex matrix. Furthermore, previous work on stabilized finite element methods for the discretization of the Helmholtz equation [15,16] suggests that a good choice for $\mathbf{S}_{bb}$ is an interface mass matrix. Hence, we propose to construct $\mathbf{S}_{bb}$ as follows

$$[\mathbf{S}_{bb}]_{lm} = \mathrm{i}k[\mathbf{M}_{bb}]_{lm} = \mathrm{i}k \int_{\Omega^1 \cap \Omega^2} \phi_l \phi_m \, \mathrm{d}\xi, \tag{8}$$

where $\mathrm{i} = \sqrt{-1}$, and ϕ_l and ϕ_m are the finite element shape functions associated with node l and node m on the interface between subdomains Ω^1 and Ω^2. Indeed, $\mathbf{M}_{bb}$ is positive definite, and therefore it can be shown that

$$\widetilde{\mathbf{K}}^s = \mathbf{K}^s - k^2\mathbf{M}^s \pm \mathrm{i}k\mathbf{M}_I^s, \quad \text{where } \mathbf{M}_I^s = \begin{bmatrix} 0 & 0 \\ 0 & \mathbf{M}_{bb} \end{bmatrix} \tag{9}$$

is non-singular for any value of k and independently of the value of the mesh size h (see Theorem A.1 in Appendix A). Furthermore, computational efficiency suggests that the matrix $\mathbf{M}_{bb}$ that arises in the regularization process should be constructed as a lumped rather than consistent mass matrix.

2.2. Interpretation in terms of subdomain interface conditions

An incomplete form of the two-subdomain formulation of the exterior Helmholtz boundary value problem (1) can be written as

$$\begin{aligned} &-\nabla^2 u^s - k^2 u^s = f^s \quad \text{in } \Omega^s, \\ &u^s = g_1^s \quad \text{on } \Gamma_{\mathrm{D}}^s, \\ &\nabla u^s \cdot v^s = g_2^s \quad \text{on } \Gamma_{\mathrm{N}}^s, \end{aligned} \tag{10}$$

where $s = 1, 2$, and the Sommerfeld condition is added for the unbounded subdomains. The above form is incomplete because it lacks two subdomain interface conditions. Two transmission conditions can be chosen as

$$\begin{aligned} &u^1 = u^2 \quad \text{on } \Omega^1 \cap \Omega^2, \\ &\frac{\partial u^1}{\partial v^1} = -\frac{\partial u^2}{\partial v^2} \quad \text{on } \Omega^1 \cap \Omega^2, \end{aligned} \tag{11}$$

where v^s denotes here the unit outward normal on the interface boundary between Ω^1 and Ω^2. However, it is well-known that the two-subdomain boundary value problem (10) equipped with the transmission conditions (11) may be ill-posed because of the existence of eigenvalues of the Laplace operator [17].

In [1,3], the authors have proposed to equip the two-subdomain exterior Helmholtz problem (10) with the alternative transmission conditions

$$\begin{aligned} \frac{\partial u^1}{\partial v^1} + \mathrm{i}ku^1 &= -\frac{\partial u^2}{\partial v^2} + \mathrm{i}ku^2 \quad \text{on } \Omega^1 \cap \Omega^2, \\ \frac{\partial u^1}{\partial v^1} - \mathrm{i}ku^1 &= -\frac{\partial u^2}{\partial v^2} - \mathrm{i}ku^2 \quad \text{on } \Omega^1 \cap \Omega^2, \end{aligned} \tag{12}$$

because in that case the subdomain problems are well posed. The above transmission conditions, which are linear combinations of the Dirichlet and Neumann interface boundary conditions (11), have inspired several DD methods (see the list given in [3]), among which we note our previous works [5,8,7].

For $\mathbf{S}_{bb} = \mathrm{i}k\mathbf{M}_{bb}$, the DD method based on the modified Lagrangian formulation (4) is equivalent to equipping the exterior Helmhotlz boundary value problem (10) with one radiation and one Dirichlet transmission conditions, and identifying each of the left and right-hand sides of the radiation condition with the *same* Lagrange multiplier field λ

$$\frac{\partial u^1}{\partial v^1} + \mathrm{i}ku^1 = -\frac{\partial u^2}{\partial v^2} + \mathrm{i}ku^2\lambda, \quad u^1 = u^2. \tag{13}$$

The first of the above two interface boundary conditions is what allows the regularization of the subdomain problems. Identifying both members of the radiation condition with λ and selecting a Dirichlet condition as a second interface boundary condition is what allows the re-use of a significant amount of techniques previously developed for the solution of elasticity problems by the mathematically optimal FETI method [10–13]. Hence, the formulation of the DD method with a single Lagrange multiplier field presented in this section differs from that of the FETI method for elasticity and plate and shell problems by the radiation transmission condition that replaces the usual Neumann interface boundary condition.

Next, we generalize the formulation of the DD method presented herein to the case of an arbitrary mesh partition with N_s subdomains.

2.3. Arbitrary mesh partitions

The modified Lagrangian corresponding to a Helmholtz problem with N_s arbitrary subdomains can be written as

$$\mathscr{L}(\mathbf{v}^s, \boldsymbol{\lambda}) = \sum_{s=1}^{s=N_s}\left(\frac{1}{2}\mathbf{v}^{s\mathrm{T}}\widetilde{\mathbf{K}}^s\mathbf{v}^s - \mathbf{f}^{s\mathrm{T}}\mathbf{v}^s\right) + \boldsymbol{\lambda}^{\mathrm{T}}\sum_{s=1}^{s=N_s}\mathbf{B}^s\mathbf{v}^s + \sum_{s=1}^{s=N_s}\sum_{\Omega^s\cap\Omega^q\neq\{\emptyset\}}\frac{1}{2}\left(\mathbf{v}_b^{s\mathrm{T}}\mathbf{S}_{bb}^{s,q}\mathbf{v}_b^s - \mathbf{v}_b^{q\mathrm{T}}\mathbf{S}_{bb}^{q,s}\mathbf{v}_b^q\right), \tag{14}$$

where $\widetilde{\mathbf{K}}^s = \mathbf{K}^s - k^2\mathbf{M}^s$ if Ω^s does not intersect the outer boundary of the computational domain, and $\widetilde{\mathbf{K}}^s = \mathbf{K}^s - k^2\mathbf{M}^s + \mathrm{i}k\mathbf{M}_{\mathrm{S}}^s$ otherwise, and $\mathbf{S}_{bb}^{s,q}$ is an interface matrix with non-zero values only on $\Omega^s \cap \Omega^q$, and constructed as the lumped mass matrix associated with the degrees of freedom lying on $\Omega^s \cap \Omega^q$

$$\mathbf{S}_{bb}^{s,q} = \epsilon^{s,q}\mathrm{i}k\mathbf{M}_{bb}^{s,q}, \qquad [\mathbf{M}_{bb}^{s,q}]_{lm} = \int_{\Omega^s\cap\Omega^q}\phi_l\phi_m\,\mathrm{d}\xi, \qquad \epsilon^{q,s} = -\epsilon^{s,q} = \pm 1. \tag{15}$$

Using a notation similar to that of Eq. (9), the Euler equations associated with the above modified Lagrangian can be written as

$$\begin{aligned} &(\widetilde{\mathbf{K}}^s + \mathrm{i}k\mathbf{M}_I^s)\mathbf{u}^s = (\mathbf{K}^s - k^2\mathbf{M}^s + \mathrm{i}k\mathbf{M}_I^s)\mathbf{u}^s = \mathbf{f}^s - \mathbf{B}^{s\mathrm{T}}\boldsymbol{\lambda}, \quad s = 1, \ldots, N_s \\ &\sum_{s=1}^{s=N_s}\mathbf{B}^s\mathbf{u}^s = 0, \end{aligned} \tag{16}$$

where

$$\mathbf{M}_I^s = \begin{bmatrix} 0 & 0 \\ 0 & \displaystyle\sum_{\Omega^s\cap\Omega^q\neq\{\emptyset\}}\epsilon^{s,q}\mathbf{M}_{bb}^{s,q} \end{bmatrix}. \tag{17}$$

From Eqs. (16) and (17) and Theorem A.1 in Appendix A, it follows that if $\mathbf{M}_I^s$ has a constant sign – that is, if $\forall q/\Omega^s \cap \Omega^q \neq \{\emptyset\}\epsilon^{s,q} = 1$, or $\forall q\Omega^s \cap \Omega^q \neq \{\emptyset\}\epsilon^{s,q} = -1$ – the subdomain problem matrix $\widetilde{\mathbf{K}}^s + \mathrm{i}k\mathbf{M}_I^s$ is non-singular for any value of k and any value of the mesh size h.

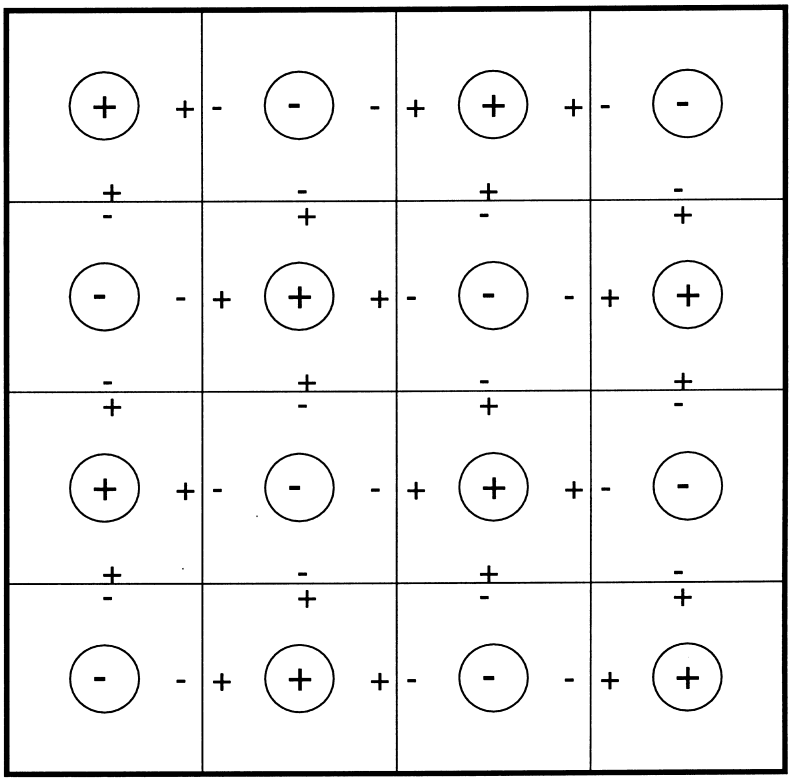

Fig. 1. Signing the edges of a checkerboard mesh partition.

When the domain Ω is partitioned in a checkerboard fashion, a red-black signing of the subdomains ensures that $\mathbf{M}_I^s$ has a constant sign along the interface boundaries of each subdomain Ω^s (Fig. 1), which guarantees that all the subdomain problems are well-posed.

When Ω is not or cannot be partitioned in a checkerboard fashion, but is rather decomposed into N_s arbitrary subdomains (Fig. 2), the following algorithm can be applied for signing the subdomains and constructing the interface mass matrices $\epsilon^{s,q}\mathrm{i}k\mathbf{M}_{bb}^{s,q}$ in a manner that guarantees that $\mathbf{M}_I^s$ has a constant sign

Step 1. Attribute arbitrary signs to all subdomains.

Step 2. Loop on the subdomains and for each subdomain, revisit the signs of the neighbors so that at least one neighbor has an opposite sign.

Step 3. Attribute the sign of a subdomain to its interface boundaries.

Step 4. Loop on the edges $\Omega^s \cap \Omega^q$. If an edge has two different signs on its two sides, construct $\mathbf{M}_{bb}^{s,q}$, and regularize $\widetilde{\mathbf{K}}^s$ with $\mathbf{S}_{bb}^{s,q} = \epsilon^{s,q}\mathrm{i}k\mathbf{M}_{bb}^{s,q}$ and $\widetilde{\mathbf{K}}^q$ with $\mathbf{S}_{bb}^{s,q} = \epsilon^{q,s}\mathrm{i}k\mathbf{M}_{bb}^{s,q}$; otherwise, set $\mathbf{S}_{bb}^{s,q} = 0$ and do not perform any regularization.

From Theorem A.1 in Appendix A, it follows that the subdomain problem matrices $\widetilde{\mathbf{K}}^s + \mathrm{i}k\mathbf{M}_I^s$ resulting from the above procedure are also non-singular.

The case of N_s arbitrary subdomains is illustrated in Fig. 2. The reader can check that because each subdomain Ω^s has at least one neighbor Ω^q with an opposite sign, it has at least one edge $\Omega^s \cap \Omega^q$ for which a regularization interface mass matrix is constructed.

2.4. The regularized FETI method for complex problems

The interface problem associated with the regularized subdomain Eq. (16) is given by

$$\mathbf{F}_I\boldsymbol{\lambda} = \mathbf{d},$$

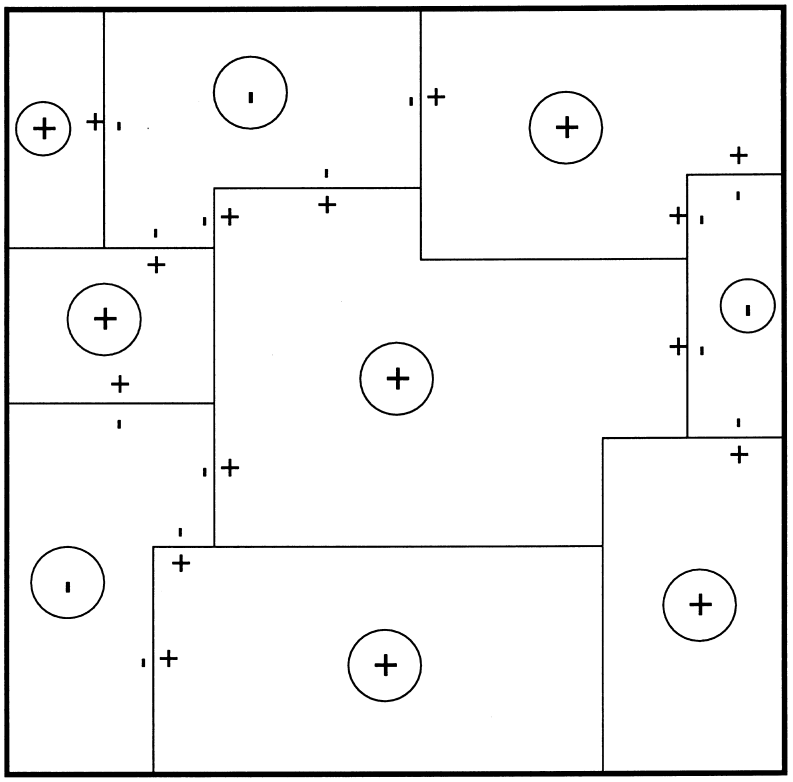

Fig. 2. Signing the edges of an irregular mesh partition.

where

$$\mathbf{F}_I = \sum_{s=1}^{s=N_s} \mathbf{B}^s (\widetilde{\mathbf{K}}^s + \mathrm{i}k\mathbf{M}_I^s)^{-1} \mathbf{B}^{s\mathrm{T}} = \sum_{s=1}^{s=N_s} \mathbf{B}^s (\mathbf{K}^s - k^2\mathbf{M}^s + \mathrm{i}k\mathbf{M}_I^s)^{-1} \mathbf{B}^{s\mathrm{T}},$$
$$\mathbf{d} = \sum_{s=1}^{s=N_s} \mathbf{B}^s (\widetilde{\mathbf{K}}^s + \mathrm{i}k\mathbf{M}_I^s)^{-1} \mathbf{M}^s. \tag{18}$$

Note that $\mathbf{F}_I$ is symmetric but not Hermitian.

Iterative algorithms such as GMRES and QMR are often applied to the solution of matrix problems arising from the discretization of the Helmholtz equation. However, these methods do not exploit the symmetry of the system matrix, and therefore perform full orthogonalization of the search directions. The conjugate residual (CR), bi-conjugate gradient (BiCG), and symmetric QMR algorithms are symmetric alternatives to these popular methods (see, for example [18]). Among these alternatives, the CR and BiCG algorithms are most attractive because of their simplicity, computational efficiency, and convergence properties [19].

Previously [8], we have proposed to solve the interface problem (18) by the CR method equipped with the "symmetric" rather than Hermitian inner product [20]. Since then, we have found that the GCR algorithm offers more robustness at the cost of a full reorthogonalization of the search directions. Such a cost is negligible compared to the cost of the solution of the subdomain problems. Therefore, in this work, we choose the GCR method for solving the interface problem (18). We refer to the resulting iterative solver as the unpreconditioned regularized FETI method for complex problems.

2.5. A two-level approach for constructing a coarse problem

The methodology we follow here for preconditioning the regularized FETI method for the exterior Helmholtz problem is based on an idea that was first proposed in [21] in the context of elastodynamics problems. This idea was also transformed in [22] into a two-level concept of the FETI method for solving efficiently various difficult elliptic problems. Essentially, we propose to precondition at each iteration the interface residual generated by the GCR algorithm, by solving an auxiliary second-level problem obtained by projecting the interface problem (18) onto a suitable coarse space.

Let $\mathbf{r}^k$ denote the kth residual associated with the solution by the GCR algorithm of the interface problem (18)

$$\mathbf{r}^k = \mathbf{d} - \mathbf{F}_I \boldsymbol{\lambda}^k. \tag{19}$$

The convergence of the regularized FETI method can be accelerated by modifying the GCR algorithm so that, at every iteration k, the interface residual $\mathbf{r}^k$ is orthogonal to a subspace represented by an interface matrix $\mathbf{Q}$

$$\mathbf{Q}^{\mathrm{T}} \mathbf{r}^k = 0. \tag{20}$$

Indeed, condition (20) is a weighted-residual weak form of $\mathbf{r}^k$. Because $\mathbf{F}_I$ is symmetric, the effect of this condition at each iteration k is to reduce the error $\mathbf{r}^k$ and accelerate convergence (see Remark 1 below). For example, if n_I denotes the size of the interface problem, constructing an interface matrix $\mathbf{Q}$ with n_I linearly independent columns guarantees that after modification to enforce at every iteration $\mathbf{Q}^{\mathrm{T}}\mathbf{r}^k = 0$, the regularized FETI method converges in one iteration. However, the subspace represented by the interface matrix $\mathbf{Q}$ must be chosen "coarse" enough to keep the overhead associated with enforcing $\mathbf{Q}^{\mathrm{T}}\mathbf{r}^k = 0$ affordable.

Eq. (20) was called in Ref. [22] an "optional admissible solution" constraint. It is a solution constraint, because

$$\mathbf{r}^k = \mathbf{d} - \mathbf{F}_I \boldsymbol{\lambda}^k = \sum_{s=1}^{s=N_s} \mathbf{B}^s \mathbf{u}^{s^k}, \tag{21}$$

which shows that $\mathbf{r}^k$ is the value at iteration k of the jump of the subdomain solutions $\mathbf{u}^{s^k}$ at the subdomain interfaces. It is an admissible constraint because it is satisfied by the exact solution. This constraint is also called an optional constraint because the regularized FETI method converges without it.

A straightforward approach for enforcing at each GCR iteration $\mathbf{Q}^{\mathrm{T}}\mathbf{r}^k = 0$ is to introduce an additional Lagrange multiplier vector of the form $\boldsymbol{\mu} = \mathbf{Q}\boldsymbol{\gamma}$ in the regularized FETI method, where $\boldsymbol{\gamma}$ is a vector of additional unknowns. More specifically, the GCR algorithm is modified so that each iterate $\boldsymbol{\gamma}$ is transformed into an iterate $\widetilde{\boldsymbol{\lambda}}^k$ as follows

$$\widetilde{\boldsymbol{\lambda}}^k = \boldsymbol{\lambda}^k + \boldsymbol{\lambda}^k = \boldsymbol{\lambda}^k + \mathbf{Q}\gamma^k, \tag{22}$$

where as before, the role of $\boldsymbol{\lambda}^k$ is to enforce at convergence $\sum_{s=1}^{s=N_s} \mathbf{B}^s \mathbf{u}^s = 0$, and the role of the correction term $\boldsymbol{\mu}^k = \mathbf{Q}\boldsymbol{\gamma}^k$ is to enforce exactly at each iteration k the optional admissible constraint $\mathbf{Q}^{\mathrm{T}}\mathbf{r}^k = 0$. Substituting Eq. (22) into Eq. (20) gives

$$\mathbf{Q}^{\mathrm{T}}\mathbf{F}_I\mathbf{Q}\boldsymbol{\gamma}^k = \mathbf{Q}^{\mathrm{T}}(\mathbf{d} - \mathbf{F}_I\boldsymbol{\lambda}^k), \tag{23}$$

which shows that at each iteration k, $\boldsymbol{\gamma}^k$ can be obtained from the solution of an auxiliary problem. This problem is called a "second-level coarse FETI" problem because:

- $\mathbf{Q}^{\mathrm{T}}\mathbf{F}_I\mathbf{Q} = \mathbf{Q}^{\mathrm{T}}(\mathbf{d} - \mathbf{F}_I\boldsymbol{\lambda}^k)$ is the projection of the regularized FETI interface problem (18) onto the subspace represented by the interface matrix $\mathbf{Q}$;
- for computational efficiency, $\mathbf{Q}$ should be constructed with as few columns as possible, and therefore the corresponding subspace is "coarse".

From Eqs. (22) and (23), it follows that $\widetilde{\boldsymbol{\lambda}}^k$ can be computed as

$$\widetilde{\boldsymbol{\lambda}}^k = \mathbf{P}\boldsymbol{\lambda}^k + \boldsymbol{\lambda}^0, \tag{24}$$

where $\mathbf{P}$ is the projector given by

$$\mathbf{P} = \mathbf{I} - \mathbf{Q}(\mathbf{Q}^{\mathrm{T}}\mathbf{F}_I\mathbf{Q})^{-1}\mathbf{Q}^{\mathrm{T}}\mathbf{F}_I \tag{25}$$

and $\boldsymbol{\lambda}^0$ is given by

$$\boldsymbol{\lambda}^0 = \mathbf{Q}(\mathbf{Q}^{\mathrm{T}}\mathbf{F}_I\mathbf{Q})^{-1}\mathbf{Q}^{\mathrm{T}}\mathbf{d}. \tag{26}$$

Substituting $\boldsymbol{\lambda}$ by $\widetilde{\boldsymbol{\lambda}}$ Eq. (24) in the interface problem (18) and premultiplying the result by $\mathbf{P}^{\mathrm{T}}$ transforms the original regularized FETI interface problem into

$$\mathbf{P}^{\mathrm{T}}\mathbf{F}_I\mathbf{P}\boldsymbol{\lambda} = \mathbf{P}^{\mathrm{T}}\mathbf{d}. \tag{27}$$

Hence, accelerating the convergence of the regularized FETI method by the introduction of the second-level FETI problem (23) can be interpreted as replacing the original interface problem (18) by the alternative interface problem (27). Furthermore, solving the symmetric complex problem (27) by the GCR algorithm can also be interpreted as solving the original symmetric interface problem (18) by a preconditioned GCR algorithm, where the preconditioner is $\mathbf{P}\mathbf{P}^{\mathrm{T}}$. The major additional computational cost entailed by this preconditioner is that associated with the construction of the reduced matrix $\mathbf{Q}^{\mathrm{T}}\mathbf{F}_I\mathbf{Q}$. This matrix has a sparsity pattern dictated by the connectivity of the subdomains and their neighbors. For a given problem, it is factored once. Furthermore, the coarse problem represented by the matrix $\mathbf{Q}^{\mathrm{T}}\mathbf{F}_I\mathbf{Q}$ needs to be solved by forward and backward substitutions only *once* in each GCR iteration, because

$$\begin{aligned}\mathbf{P}^{\mathrm{T}}\mathbf{F}_I\mathbf{P} &= (\mathbf{I} - \mathbf{F}_I\mathbf{Q}(\mathbf{Q}^{\mathrm{T}}\mathbf{F}_I\mathbf{Q})^{-1}\mathbf{Q}^{\mathrm{T}})\mathbf{F}_I(\mathbf{I} - \mathbf{Q}(\mathbf{Q}^{\mathrm{T}}\mathbf{F}_I\mathbf{Q})^{-1}\mathbf{Q}^{\mathrm{T}}\mathbf{F}_I) = \mathbf{F}_I - \mathbf{F}_I\mathbf{Q}(\mathbf{Q}^{\mathrm{T}}\mathbf{F}_I\mathbf{Q})_I^{-1}\mathbf{Q}^{\mathrm{T}}\mathbf{F}_I \\ &= \mathbf{F}_I\mathbf{P},\end{aligned} \tag{28}$$

which implies that only one projection step is required at each GCR iteration implementing $\mathbf{P}^{\mathrm{T}}$. The effect of such time is relatively negligible.

In summary, the convergence of the regularized FETI method can be accelerated by enforcing at each GCR iteration an optional admissible solution constraint of the form $\mathbf{Q}^{\mathrm{T}}\mathbf{r}^k = 0$. This requires transforming each iterate $\boldsymbol{\lambda}^k$ into the iterate $\widetilde{\boldsymbol{\lambda}}^k$ as described in Eqs. (22)–(26), which in turn requires solving at each iteration the second-level FETI problem (23). We refer to the resulting algorithm as the two-level FETI-H method, where the letter H stands for the exterior Helmholtz problem. If the number of columns of $\mathbf{Q}$ is kept sufficiently small, the second-level problem becomes a coarse problem. It couples all the subdomain computations, and therefore provides a mechanism for propagating the error globally, and ensuring the numerical scalability of the regularized FETI method with respect to the number of subdomains.

The FETI-H method is summarized in Box 1 where the parentheses around a quantity of the form $\mathbf{F}_I\mathbf{s}$, where $\mathbf{s}$ is a generic interface vector, are used to imply that $(\mathbf{F}_I\mathbf{s})$ is a vector variable and *not* a matrix–vector computation, and the $*$ superscript designates the transpose of the complex conjugate of a quantity. The reader can check that, as described in Box 1, the FETI-H method performs a single projection of the form $\mathbf{P}\mathbf{s}$ and a single matrix–vector product of the form $\mathbf{F}_I\mathbf{t}$ per iteration. In this work, the solution of the second-level coarse problem is parallelized at the algebraic level, but the remainder of the FETI-H computations are parallelized at the subdomain level (subdomain-by-subdomain parallel computations).

Remark 1. *A conjugate gradient type of method applied to the solution of a problem of size n_I and of the form $\mathbf{F}_I\boldsymbol{\lambda} = \mathbf{d}$ can be viewed as an algorithm for minimizing over a Krylov subspace the $\mathbf{A}$-norm of the error $\boldsymbol{\lambda} - \boldsymbol{\lambda}^k$* [23]. *When $\mathbf{F}_I$ is symmetric positive definite, $\mathbf{A}$ can be set to $\mathbf{A} = \mathbf{F}_I$, in which case the method minimizes $\|\boldsymbol{\lambda} - \boldsymbol{\lambda}^k\|_{\mathbf{F}_I}$. Given a matrix $\mathbf{Q}$ of full column rank n_Q, if at each iteration $\boldsymbol{\lambda}^k$ is replaced by $\boldsymbol{\lambda}^k + \mathbf{Q}\boldsymbol{\mu}^k$ where $\boldsymbol{\mu}^k$ is computed as to minimize $\|\boldsymbol{\lambda} - (\boldsymbol{\lambda}^k + \mathbf{Q}\boldsymbol{\mu}^k)\|_{\mathbf{F}_I}$, then the finite termination property of the conjugate gradient method is improved from n_I iterations to $n_I - n_Q$ iterations. This suggests that enriching the space of search directions of the conjugate gradient method by the range of $\mathbf{Q}$ accelerates convergence. The reader can check that solving the latter minimization problem leads to the same Eqs.* (23)–(26) *that are obtained when the optional constraint $\mathbf{Q}^{\mathrm{T}}\mathbf{r}^k = 0$ is enforced at each iteration k (see* [24] *for a rigorous derivation). Hence, enforcing $\mathbf{Q}^{\mathrm{T}}\mathbf{r}^k = 0$ at each iteration accelerates convergence. Here, $\mathbf{F}_I$ is complex and not Hermitian. For this*

reason, $\mathbf{A}$ *should be in theory set to* $\mathbf{A} = \mathbf{F}_I^* \mathbf{F}_I$ (*indeed, the GCR algorithm minimizes* $||\boldsymbol{\lambda} - \boldsymbol{\lambda}^k||_{\mathbf{F}_I^* \mathbf{F}_I}$), *and* $\mathbf{Q}^{\mathrm{T}} \mathbf{r}^k = 0$ *should be replaced by* $\mathbf{Q}^* \mathbf{F}_I^* \mathbf{r}^k = 0$. *This is done in Section* 3.3. *When* $\mathbf{F}_I$ *is not Hermitian but symmetric, we still found out in practice that enforcing* $\mathbf{Q}^{\mathrm{T}} \mathbf{r}^k = 0$ *accelerates convergence*.

Box 1. The two-level FETI-H method for exterior Helmholtz problems

1. Initialize

$$\begin{aligned}
\lambda^0 &= \mathbf{Q}\ [\mathbf{Q}^{\mathrm{T}} \mathbf{F}_I \mathbf{Q}]^{-1} \mathbf{d}, \\
\mathbf{r}^0 &= \mathbf{d} - \mathbf{F}_I \lambda^0, \\
\mathbf{y}^0 &= \mathbf{P} \mathbf{r}^0, \\
\mathbf{p}^0 &= \mathbf{y}^0, \\
(\mathbf{F}_I \mathbf{p})^0 &= \mathbf{F}_I \mathbf{p}^0.
\end{aligned}$$

2. Iterate $k = 1, 2, \ldots$ until convergence

$$\begin{aligned}
\zeta^k &= (\mathbf{F}_I \mathbf{p})^{k-1^*} \mathbf{r}^{k-1} / (\mathbf{F}_I \mathbf{p})^{k-1^*} (\mathbf{F}_I \mathbf{p})^{k-1}, \\
\boldsymbol{\lambda}^k &= \boldsymbol{\lambda}^{k-1} - \zeta^k \mathbf{p}^{k-1}, \\
\mathbf{r}^k &= \mathbf{r}^{k-1} - \zeta^k (\mathbf{F}_I \mathbf{p})^{k-1}, \\
\mathbf{y}^k &= \mathbf{P} \mathbf{r}^k, \\
(\mathbf{F}_I \mathbf{y})^k &= \mathbf{F}_I \mathbf{y}^k, \\
\mathbf{p}^k &= \mathbf{y}^k + \sum_{i=0}^{i=k-1} \frac{(\mathbf{F}_I \mathbf{p})^{i^*} (\mathbf{F}_I \mathbf{y})^k}{(\mathbf{F}_I \mathbf{p})^{i^*} (\mathbf{F}_I \mathbf{p})^i} \mathbf{p}^i, \\
(\mathbf{F}_I \mathbf{P})^k &= (\mathbf{F}_I \mathbf{y})^k + \sum_{i=0}^{i=k-1} \frac{(\mathbf{F}_I \mathbf{p})^{i^*} (\mathbf{F}_I \mathbf{y})^k}{(\mathbf{F}_I \mathbf{p})^{i^*} (\mathbf{F}_I \mathbf{p})^i} (\mathbf{F}_I \mathbf{p})^i.
\end{aligned} \tag{29}$$

2.6. Constructing the coarse basis with planar waves

To complete the description of the FETI-H method, it remains to specify the choice of the coarse space represented by the matrix $\mathbf{Q}$. Given that the solution of the exterior Helmholtz problem can be approximated by the superposition of planar waves, and that the residual $\mathbf{r}^k$ measures at each iteration k the jump of the solution at the subdomain interfaces, we propose to base our coarse problem on planar waves. More specifically, we choose

$$\mathbf{Q}_j(-) = \mathrm{e}^{\mathrm{i}k\boldsymbol{\theta}_j^{\mathrm{T}}(-)\mathbf{x}(-)}; \quad \theta_j = (j-1) \times \frac{2\Pi}{N_\theta}, \quad j = 1, \ldots, N_\theta; \quad N_\theta \text{ even}, \tag{30}$$

where $\mathbf{Q}_j(-)$ denotes the jth column of $\mathbf{Q}$ evaluated at the grid point designated by the – label, $\mathbf{x}(-)$ denotes the vector of nodal point coordinates evaluated at the grid point –, $\boldsymbol{\theta}_j(-)$ is the unitary directional vector located at the grid point – and intersecting the horizontal axis with an angle equal to θ_j (see Fig. 3, and N_θ is the number of directional wave propagation vectors *per grid point* and has a priori the same value at all grid points. Note that N_θ is chosen as an even integer in order to include in $\mathbf{Q}$ both directions $+\theta_j$ and $-\theta_j$.

Furthermore, we construct $\mathbf{Q}$ at the subdomain level to allow (a) different superpositions of the planar waves at different regions in the mesh, and (b) a better parallel implementation. In other words, we form $\mathbf{Q}$ as follows

$$\mathbf{Q} = [\mathbf{Q}^1 \quad \ldots \quad \mathbf{Q}^s \quad \ldots \quad \mathbf{Q}^{N_s}], \tag{31}$$

where $\mathbf{Q}^s$ has nonzero entries only on the points located on the interface boundary of Ω^s. If follows that the number of columns of $\mathbf{Q}$ is equal to $N_s \times N_\theta$. Depending on the parameters of the problem to be solved, $\mathbf{Q}$

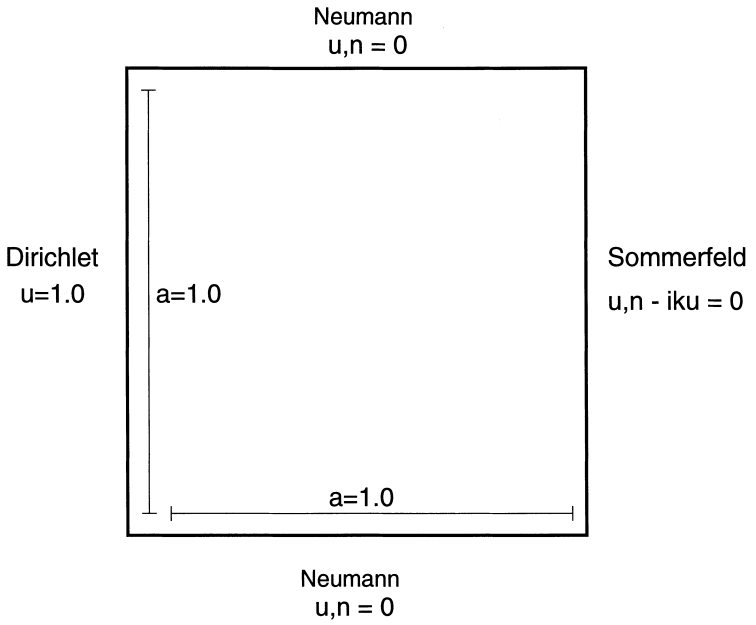

Fig. 3. Representation of planer waves.

may not have a full column rank. In that case, the second-level problem matrix $\mathbf{Q}^{\mathrm{T}}\mathbf{F}_I\mathbf{Q}$ is singular, and its linearly dependent columns are filtered out during its factorization.

2.7. Convergence properties of the regularized FETI method

An interesting property of the regularized FETI method for Helmholtz problems is that, even in the absence of a preconditioner, it is numerically scalable with respect to the mesh size h. This is a rather surprising result given that the regularized FETI method for Laplace problems requires a preconditioner in order to scale with the problem size [11]. Here, we highlight this property with a guided wave problem and investigate the effects on convergence of the subdomain size H and the wavenumber k.

For this purpose, we consider the guided wave problem depicted in Fig. 4. First, we set the wavenumber to $ka = 20$. We construct four different uniform meshes corresponding to $h = 1/100$, $h = 1/150$, $h = 1/200$, and $h = 1/250$, and discretize the Helmholtz equation by $Q1$ finite elements. The coarsest of these four

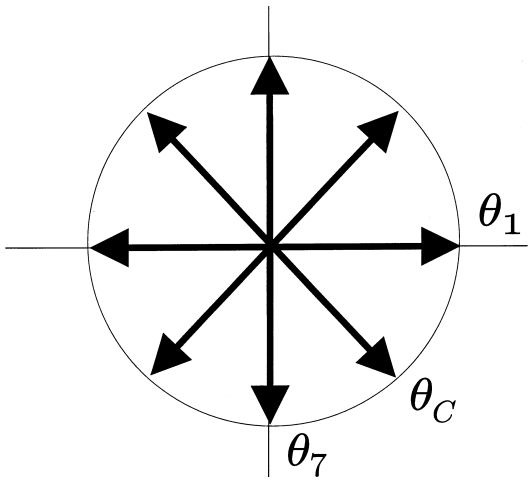

Fig. 4. The guided wave problem.

meshes contains 31 elements per wave length. We partition each mesh into 5×5 subdomains, and apply the regularized FETI method to the solution of the resulting systems of equations. In all cases and throughout the remainder of this paper, we use the following convergence criterion

$$\|\widetilde{\mathbf{K}}\mathbf{u} - \mathbf{f}\| \leqslant 10^{-6}\|\mathbf{f}\|, \tag{32}$$

where $\|\mathbf{f}\|$ denotes here the modulus of the complex number $\mathbf{f}^*\mathbf{f}$. We report in Table 1 the obtained performance results. These demonstrate that even in the absence of a preconditioner, the regularized FETI method for Helmholtz problems is scalable with respect to the mesh size h.

Next, we focus on the case $h = 1/200$ and partition the corresponding mesh into 2×2, 4×4 and 5×5 subdomains. In that case, the results reported in Table 2 show that the performance of the unpreconditioned regularized FETI method does not scale with the number of subdomains.

Finally, we fix the mesh size to $h = 1/315$, partition Ω into 5×5 subdomains, and consider three different wavenumbers corresponding to $ka = 20$, $ka = 40$ and $ka = 60$. Note that for the highest frequency case, the mesh contains 33 elements per wave length. The performance results we report in Table 3 demonstrate that in the absence of a preconditioner, the number of iterations for convergence of the regularized FETI method increases sublinearly with the wavenumber.

In summary, in the absence of a preconditioner, the FETI based DD method with a single Lagrange multiplier field presented in this section is scalable with respect to mesh size h, but not with respect to the subdomain size H and the wavenumber k. Next, we investigate the convergence properties of this method equipped with the preconditioner described in Sections 2.5 and 2.6 – that is, the FETI-H method.

2.8. Convergence properties of the FETI-H method

We consider again the guided wave problem depicted in Fig. 4. First, we set $ka = 32$ and $h = 1/315$ (62 elements per wave length), and generate several $1/H \times 1/H$ mesh partitions with 25, 49, and 81 subdo-

Table 1
The guided wave problem – $ka = 20$ – $N_s = 25$ (performance results of the unpreconditioned regularized FETI method)

h	Number of iterations
1/100	91
1/150	94
1/200	96
1/250	96

Table 2
The guided wave problem – $ka = 20$ – $N_s = 1/200$ (performance results of the unpreconditioned regularized FETI method)

h	Number of iterations
4	31
16	71
25	96

Table 3
The guided wave problem – $h = 1/315$ – $N_s = 25$ (performance results of the unpreconditioned regularized FETI method)

h	Number of iterations
20	97
40	136
60	167

Table 4
The guided wave problem – $ka = 32$ – $h = 1/315$ (performance results of the FETI method)

N_θ	N_s	Size of the coarse problem	Total size of the problem	Number of iterations
4	25	88	99225	41
4	49	180	99225	49
4	81	304	99225	41
8	25	172	99225	20
8	49	341	99225	17
8	81	532	99225	26
16	25	224	99225	17
16	49	426	99225	19
16	81	606	99225	28

mains. For each case, we consider three different coarse problems with N_θ equal to 4, 8 and 16, respectively. We report in Table 4 the corresponding performance results. Note that in this and all subsequent tables, the size of the coarse problem is computed as the number of linearly independent columns found during the factorization of the second-level problem matrix $\mathbf{Q}^{\mathrm{T}}\mathbf{F}_I\mathbf{Q}$. Hence, this size is less or equal to $N_\theta \times N_s$.

The information summarized in Table 4 shows that:

- For any value of N_θ, the FETI-H method is scalable with respect to the subdomain size H.
- For a constant size ($N_s \times N_\theta$) of the coarse problem, the best iteration count is obtained in general for the case with a larger N_θ and smaller number of subdomains. This suggests the existence of a threshold value

Table 5
The guided wave problem – $h = 1/315$ (performance results of the FETI-H method)

Ka	N_θ	N_s	Size of the coarse problem	Total size of the problem	Number of iterations
20	4	25	88	99225	31
20	4	49	180	99225	30
20	4	81	304	99225	27
20	8	25	176	99225	18
20	8	49	354	99225	19
20	8	81	600	99225	17
20	16	25	262	99225	18
20	16	49	471	99225	19
20	16	81	713	99225	18
40	4	25	88	99225	69
40	4	49	180	99225	54
40	4	81	304	99225	59
40	8	25	176	99225	25
40	8	49	354	99225	22
40	8	81	600	99225	22
40	16	25	262	99225	18
40	16	49	471	99225	19
40	16	81	713	99225	22
60	4	25	88	99225	138
60	4	49	180	99225	137
60	4	81	304	99225	100
60	8	25	176	99225	48
60	8	49	354	99225	40
60	8	81	600	99225	21
60	16	25	262	99225	17
60	16	49	471	99225	16
60	16	81	713	99225	16

of N_θ below which increasing the size of the coarse problem by increasing the number of subdomains is not effective, at least from an iteration count viewpoint.
- In all cases, fast convergence is achieved with a relatively small coarse problem.

Next, we perform similar computations but for three different values of the wavenumber corresponding to $ka = 20$, $ka = 40$, and $ka = 60$. We report the obtained performance results in Table 5. These results are impressive and confirm the scalability of the FETI-H method with respect to the number of subdomains. Furthermore, they show that scalability with respect to the wavenumber k can also be achieved, not necessarily by increasing the size of the coarse problem, but more importantly by increasing the value of N_θ. For example, the case where $ka = 20$ is solved in 18 iterations when $N_\theta = 16$ directions, $N_s = 25$ subdomains, and the size of the coarse problem is equal to 262. The case where $ka = 60$ can be solved in 16 iterations using the same parameters.

3. Domain decomposition with two Lagrange multiplier fields

Another approach for regularizing the subdomain problems that is independent of the pattern of the mesh decomposition is to equip the FETI method with two Lagrange multiplier fields as described in this section.

3.1. Revisiting the regularization procedure for arbitrary mesh partitions

For arbitrary mesh partitions, the specific treatment of the subdomain interfaces described in Section 2.3, which is designed for ensuring a constant sign of the regularizing matrix $\mathbf{M}_I^s$, results from the fact that the FETI-H method considers only one normal and therefore employs only one Lagrange multiplier per mesh partition interface. Here, we present an alternative to this treatment that consists in defining a unique solution $\mathbf{u}_I$ at the subdomain interfaces, and introducing two Lagrange multipliers at each interface between two subdomains Ω^s and Ω^q: the objective of the first Lagrange multiplier is to enforce the compatibility between $\mathbf{u}_b^s$ and the corresponding component of $\mathbf{u}_I$, and that of the second Lagrange multiplier field is to enforce the compatibility between $\mathbf{u}_b^q$ and the corresponding component of $\mathbf{u}_I$. Such a strategy, which can also be viewed as introducing two different normals at each interface (one on each side), is often referred to in the domain decomposition literature as a three-field method [25] (two Lagrange multiplier fields and $\mathbf{u}_I$). We describe this alternative approach first in the context of a two-subdomain problem, then generalize it to arbitrary mesh partitions.

First, we consider the case of a two-subdomain problem and denote by $\mathbf{u}_I$ the trace of the global solution on the interface boundary $\Gamma_I = \Omega^1 \cap \Omega^2$. The classical Lagrangian associated with a two-subdomain problem where both normals are considered at the interface boundary can be written as

$$L(\mathbf{v}^1, \mathbf{v}^2, \boldsymbol{\lambda}^1, \boldsymbol{\lambda}^2, \mathbf{v}_I) = \frac{1}{2}\mathbf{v}^{1\mathrm{T}}\widetilde{\mathbf{K}}^1\mathbf{v}^1 - \mathbf{f}^{1\mathrm{T}}\mathbf{v}^1 + \frac{1}{2}\mathbf{v}^{2\mathrm{T}}\widetilde{\mathbf{K}}^2\mathbf{v}^2 - \mathbf{f}^{2\mathrm{T}}\mathbf{v}^2 + \boldsymbol{\lambda}^{1\mathrm{T}}\left(\mathbf{v}_b^1 - \mathbf{v}_I\right) + \boldsymbol{\lambda}^{2\mathrm{T}}\left(\mathbf{v}_b^2 - \mathbf{v}_I\right). \tag{33}$$

Using the same partitioning as in Eq. (3), the Euler equations associated with the above Lagrangian can be written as

$$\begin{aligned}
&\widetilde{\mathbf{K}}^1\mathbf{u}^1 = \mathbf{f}^1 - \begin{bmatrix} 0 \\ \boldsymbol{\lambda}^1 \end{bmatrix},\\
&\widetilde{\mathbf{K}}^2\mathbf{u}^2 = \mathbf{f}^2 - \begin{bmatrix} 0 \\ \boldsymbol{\lambda}^2 \end{bmatrix},\\
&\mathbf{u}_b^1 - \mathbf{u}_I = 0,\\
&\mathbf{u}_b^2 - \mathbf{u}_I = 0,\\
&-\boldsymbol{\lambda}^1 - \boldsymbol{\lambda}^2 = 0.
\end{aligned} \tag{34}$$

The interface unknown $\mathbf{u}_I$ can be eliminated by subtracting the fourth from the third of Eq. (34), which transforms the Euler equations into

$$
\begin{aligned}
&\widetilde{\mathbf{K}}^1\mathbf{u}^1 = \mathbf{f}^1 - \begin{bmatrix} 0 \\ \boldsymbol{\lambda}^1 \end{bmatrix},\\
&\widetilde{\mathbf{K}}^2\mathbf{u}^2 = \mathbf{f}^2 - \begin{bmatrix} 0 \\ \boldsymbol{\lambda}^2 \end{bmatrix},\\
&\mathbf{u}_b^1 - \mathbf{u}_I = 0,\\
&-\boldsymbol{\lambda}^1 - \boldsymbol{\lambda}^2 = 0.
\end{aligned}
\tag{35}
$$

The interpretation of the above system of equations is straightforward. The first two of Eq. (35) state that u^s, $s = 1, 2$, is solution of a Helmholtz problem defined in Ω^s with Neumann boundary conditions $(\partial u^s/\partial v^s) = -\lambda^s$ on Γ_I, and the third and fourth of Eq. (35) are the usual continuity equations of the solutions u^s and their normal derivatives $(\partial u^s/\partial v^s)$. Hence, the stationary point of the Lagrangian (33) is composed of u^1 and u^2 that are the restrictions of the solution u of problem (2) to the subdomains Ω^1 and Ω^2, respectively.

In order to regularize the local problems governed by $\widetilde{\mathbf{K}}^1$ and $\widetilde{\mathbf{K}}^2$, we follow the same procedure as in Section 2.1 and replace the Lagrangian (33) by the following modified Lagrangian

$$
\begin{aligned}
\mathscr{L}(\mathbf{v}^1, \mathbf{v}^2, \boldsymbol{\lambda}^1, \boldsymbol{\lambda}^2, \mathbf{v}_I) = L(\mathbf{v}^1, \mathbf{v}^2, \boldsymbol{\lambda}^1, \boldsymbol{\lambda}^2, \mathbf{v}_I) &+ \frac{1}{2}\left(\mathbf{v}_b^{1^{\mathrm{T}}}\mathbf{S}_{bb}\mathbf{v}_b^1\right) - \frac{1}{2}\left(\mathbf{v}_I^{\mathrm{T}}\mathbf{S}_{bb}\mathbf{v}_I\right)\\
&+ \frac{1}{2}(\mathbf{v}_b^{2^{\mathrm{T}}}\mathbf{S}_{bb}\mathbf{v}_b^2) - \frac{1}{2}(\mathbf{v}_I^{\mathrm{T}}\mathbf{S}_{bb}\mathbf{v}_I),
\end{aligned}
\tag{36}
$$

where $\mathbf{S}_{bb}$ is some interface matrix. We remind the reader that finding the stationary points $\mathbf{u}^1$ and $\mathbf{u}^2$ of the modified Lagrangian (36) is equivalent to solving problem (2), because the quantities added to L vanish when the Lagrange multipliers enforce the continuity equations $\mathbf{v}_b^1 = \mathbf{v}_b^2 = \mathbf{v}_I$.

The Euler equations associated with the modified Lagrangian (36) are given by

$$
\begin{aligned}
&(\widetilde{\mathbf{K}}^1 + \mathbf{S}_I^1)\mathbf{u}^1 = \mathbf{f}^1 - \begin{bmatrix} 0 \\ \boldsymbol{\lambda}^1 \end{bmatrix},\\
&(\widetilde{\mathbf{K}}^2 + \mathbf{S}_I^2)\mathbf{u}^2 = \mathbf{f}^2 - \begin{bmatrix} 0 \\ \boldsymbol{\lambda}^2 \end{bmatrix},\\
&\mathbf{u}_b^1 - \mathbf{u}_I = 0,\\
&\mathbf{u}_b^2 - \mathbf{u}_I = 0,\\
&-\boldsymbol{\lambda}^1 - \boldsymbol{\lambda}^2 - 2\mathbf{S}_{bb}\mathbf{u}_I = 0,
\end{aligned}
\tag{37}
$$

where $\mathbf{S}_I^s$, $s = 1, 2$, is the same matrix as in Eq. (5). Eliminating $\mathbf{u}_I$ from the above system of equations replaces the continuity equations by

$$
\begin{aligned}
&\boldsymbol{\lambda}^1 + \boldsymbol{\lambda}^2 + 2\mathbf{S}_{bb}\mathbf{u}_b^1 = 0,\\
&\boldsymbol{\lambda}^1 + \boldsymbol{\lambda}^2 + 2\mathbf{S}_{bb}\mathbf{u}_b^2 = 0.
\end{aligned}
\tag{38}
$$

Using the same arguments as in Section 2.1, we choose the regularizing matrix as $\mathbf{S}_{bb} = \mathrm{i}k\mathbf{M}_{bb}$, which transforms the governing subdomain equations into

$$
\begin{aligned}
&(\widetilde{\mathbf{K}}^1 + \mathrm{i}k\mathbf{M}_I^1)\mathbf{u}^1 = \mathbf{f}^1 - \begin{bmatrix} 0 \\ \boldsymbol{\lambda}^1 \end{bmatrix},\\
&(\widetilde{\mathbf{K}}^2 + \mathrm{i}k\mathbf{M}_I^2)\mathbf{u}^2 = \mathbf{f}^2 - \begin{bmatrix} 0 \\ \boldsymbol{\lambda}^2 \end{bmatrix},\\
&\boldsymbol{\lambda}^1 + \boldsymbol{\lambda}^2 + 2\mathrm{i}k\mathbf{M}_{bb}\mathbf{u}_b^1 = 0,\\
&\boldsymbol{\lambda}^1 + \boldsymbol{\lambda}^2 + 2\mathrm{i}k\mathbf{M}_{bb}\mathbf{u}_b^2 = 0,
\end{aligned}
\tag{39}
$$

where $\mathbf{M}_I^s$ is the same matrix as in Eq. (9).

The reader can check that the above system of equations can be interpreted as follows. The first two of Eq. (39) correspond to the discretization of two subdomain Helmholtz problems with the following radiation boundary conditions on the interface boundary

$$\begin{aligned} &\frac{\partial u^1}{\partial v^1} + \mathrm{i}ku^1 = -\lambda^1 \quad \text{on } \Omega^1 \cap \Omega^2, \\ &\frac{\partial u^2}{\partial v^2} + \mathrm{i}ku^2 = -\lambda^2 \quad \text{on } \Omega^2 \cap \Omega^1, \end{aligned} \tag{40}$$

and therefore the last two of equations of (39) arise from the discretization of the following transmission conditions

$$\begin{aligned} &\frac{\partial u^1}{\partial v^1} + \mathrm{i}ku^1 = -\frac{\partial u^2}{\partial v^2} + \mathrm{i}ku^2 \quad \text{on } \Omega^1 \cap \Omega^2, \\ &\frac{\partial u^2}{\partial v^2} + \mathrm{i}ku^2 = -\frac{\partial u^1}{\partial v^1} + \mathrm{i}ku^1 \quad \text{on } \Omega^2 \cap \Omega^1. \end{aligned} \tag{41}$$

The reader can also observe that the above transmission conditions are equivalent to the basic transmission conditions (11).

Let $\mathbf{B}_{\Gamma_I}$ denote the Boolean matrix associated with the partitioning introduced in Eq. (3). For a two-subdomain problem, $\mathbf{B}_{\Gamma_I}$ can be written as

$$\mathbf{B}_{\Gamma_I} = [0 \quad \mathbf{I}]. \tag{42}$$

Eliminating $\mathbf{u}^1$ and $\mathbf{u}^2$ from Eq. (39) leads to an interface problem of the form

$$\mathbf{F}_I \boldsymbol{\lambda} = \mathbf{d},$$

where

$$\begin{aligned} \mathbf{F}_I &= \begin{bmatrix} \mathbf{I} - 2\mathrm{i}k\mathbf{M}_{bb}\mathbf{B}_{\Gamma_I}(\widetilde{\mathbf{K}}^1 + \mathrm{i}k\mathbf{M}_I^1)^{-1}\mathbf{B}_{\Gamma_I}^{\mathrm{T}} & \mathbf{I} \\ \mathbf{I} & \mathbf{I} - 2\mathrm{i}k\mathbf{M}_{bb}\mathbf{B}_{\Gamma_I}(\widetilde{\mathbf{K}}^2 + \mathrm{i}k\mathbf{M}I^2)^{-1}\mathbf{B}_{\Gamma_I}^{\mathrm{T}} \end{bmatrix}, \\ \boldsymbol{\lambda} &= \begin{bmatrix} \boldsymbol{\lambda}^1 \\ \boldsymbol{\lambda}^2 \end{bmatrix}, \\ \mathbf{d} &= \begin{bmatrix} -2\mathrm{i}k\mathbf{M}_{bb}\mathbf{B}\Gamma_I(\widetilde{\mathbf{K}}^1 + \mathrm{i}k\mathbf{M}_I^1)^{-1}\mathbf{f}^1 \\ -2\mathrm{i}k\mathbf{M}_{bb}\mathbf{B}\Gamma_I(\widetilde{\mathbf{K}}^2 + \mathrm{i}k\mathbf{M}_I^2)^{-1}\mathbf{f}^2 \end{bmatrix}, \end{aligned} \tag{43}$$

which completes the formulation of a regularized three-field DD method for a two-subdomain Helmholtz problem. Note that the above interface problem is not Hermitian. Unlike the interface problem (18) associated with the regularized FETI method with one field of Lagrange multipliers (see Section 2.4), it is not symmetric either. Note also that even though the regularized three-field DD method described herein involves twice as many Lagrange multiplier unknowns as the regularized FETI method, in both methods, each matrix–vector product of the form $\mathbf{F}\boldsymbol{\lambda}$ incurs only one pair of forward and backward substitutions per subdomain.

Next, we extend our regularized three-field DD method to the case of an arbitrary mesh partition with $N_s > 2$ subdomains. For this purpose, we partition the interface boundary Γ_I into interface edges Γ_I^j using the following guidelines:

- an interface edge is defined as a collection of connecting interface nodes;
- each interface node is assigned to one and only one interface edge.

In particular, we treat a crosspoint as an interface edge with a single interface node. For each interface edge Γ_I^j, we define for each subdomain Ω^s that intersects Γ_I^j a Boolean matrix $\mathbf{B}_{\Gamma_I^j}^s$ by

$$\mathbf{u}_b^s \,|_{\Gamma_I^j} = \mathbf{B}_{\Gamma_I^j}^s \mathbf{u}^s. \tag{44}$$

The modified Lagrangian associated with the proposed regularized three-field DD method can then be written as

$$\mathscr{L}\left(\mathbf{v}^s, \mathbf{v}_I^j, \boldsymbol{\lambda}_{\Gamma_I^j}^s\right) = \sum_{s=1}^{s=N_s}\left(\frac{1}{2}\mathbf{v}^{s\mathrm{T}}\widetilde{\mathbf{K}}^s\mathbf{v}^s - \mathbf{v}^{s\mathrm{T}}\mathbf{f}^s\right) + \sum_{s=1}^{s=N_s}\sum_{\Gamma_I^j\subset\Omega^s}\boldsymbol{\lambda}_{\Gamma_I^j}^{s\mathrm{T}}\left(\mathbf{B}_{\Gamma_I^j}^s\mathbf{v}^s - \mathbf{v}_I^j\right)$$
$$+ \sum_{s=1}^{s=N_s}\sum_{\Gamma_I^j\subset\Omega^s}\frac{1}{2}\left(\mathbf{v}^{s\mathrm{T}}\mathbf{B}_{\Gamma_I^j}^{s\mathrm{T}}\left[\mathrm{i}k\mathbf{M}_{bb}^{\Gamma_I^j}\right]\mathbf{B}_{\Gamma_I^j}^s\mathbf{v}^s - \mathbf{v}_I^{j\mathrm{T}}\left[\mathrm{i}k\mathbf{M}_{bb}^{\Gamma_I^j}\right]\mathbf{v}_I^j\right), \tag{45}$$

where $\boldsymbol{\lambda}_{\Gamma_I^j}^s$ is the vector of Lagrange multipliers introduced at the interface edge Γ_I^j on the side of subdomain Ω^s, $\mathbf{v}_I^j$ is the restriction of $\mathbf{v}_I$ to Γ_I^j, and $\mathbf{M}_{bb}^{\Gamma_I^j}$ is the same matrix as in Eq. (15) with $\Omega^q \cap \Omega^q = \Gamma_I^j$. The Euler equations associated with the above modified Lagrangian are given by

$$\left(\widetilde{\mathbf{K}}^s + \sum_{\Gamma_I^j\subset\Omega^s}\mathbf{B}_{\Gamma_I^j}^{s\mathrm{T}}\left[\mathrm{i}k\mathbf{M}_{bb}^{\Gamma_I^j}\right]\mathbf{B}_{\Gamma_I^j}^s\right)\mathbf{u}^s = \mathbf{f}^s - \sum_{\Gamma_I^l\subset\Omega^s}\mathbf{B}_{\Gamma_I^l}^{s\mathrm{T}}\boldsymbol{\lambda}_{\Gamma_I^l}^s, \quad s = 1,\ldots N_s,$$
$$\mathbf{B}_{\Gamma_I^j}^s\mathbf{u}^s - \mathbf{u}_I^j = 0 \quad \forall\Gamma_j, \quad \forall\Omega^s \supset \Gamma_j, \tag{46}$$
$$\sum_{\Omega^q\supset\Gamma_I^j}\left(\boldsymbol{\lambda}_{\Gamma_I^j}^q + \left[\mathrm{i}k\mathbf{M}_{bb}^{\Gamma_I^j}\right]\mathbf{u}_I^j\right) = 0 \quad \forall\Gamma_I^j,$$

and can be transformed into the following interface problem

$$\sum_{\Omega^q\supset\Gamma_I^j}\left(\boldsymbol{\lambda}_{\Gamma_j}^q - \left[\mathrm{i}k\mathbf{M}_{bb}^{\Gamma_I^j}\right]\mathbf{B}_{\Gamma_j}^s\left(\widetilde{\mathbf{K}}^s + \left(\sum_{\Gamma_I^m\subset\Omega^s}B_{\Gamma_I^m}^{s\mathrm{T}}\left[\mathrm{i}k\mathbf{M}_{bb}^{\Gamma_I^m}\right]B_{\Gamma_I^m}^s\right)\right)^{-1}\sum_{\Gamma_I^l\subset\Omega^s}B_{\Gamma_I^l}^{s\mathrm{T}}\lambda_{\Gamma_I^l}^s\right)$$
$$= -\sum_{\Omega_q\supset\Gamma_I^j}\left[\mathrm{i}k\mathbf{M}_{bb}^{\Gamma_I^j}\right]\mathbf{B}_{\Gamma_j}^s\left(\widetilde{\mathbf{K}}^s + \left(\sum_{\Gamma_I^m\subset\Omega^s}B_{\Gamma_I^m}^{s\mathrm{T}}\left[\mathrm{i}k\mathbf{M}_{bb}^{\Gamma_I^m}\right]B_{\Gamma_I^m}^s\right)\right)^{-1}\mathbf{f}^s \quad \forall\Gamma_I^j, \quad \forall\Omega^s \supset \Gamma_I^j \tag{47}$$

This interface problem can also be written as $\mathbf{F}\boldsymbol{\lambda} = \mathbf{d}$, where $\mathbf{F}$ is neither Hermitian nor symmetric.

3.2. The regularized FETI method with two Lagrange multiplier fields

The GMRES and ORTHODIR algorithms [18] are the methods of choice for solving iteratively the interface problem (47) which, as stated earlier, is neither Hermitian nor symmetric. Given that ORTHODIR is simpler to implement than GMRES, and that the number of interface unknowns in a subdomain is usually much smaller than the number of words required for storing the factors of the subdomain problem matrix, we choose to solve the complex interface problem (47) by an ORTHODIR scheme with full orthogonalization. We refer to the resulting iterative solver as the unpreconditioned regularized FETI method with two Lagrange multiplier fields for complex problems, and denote it by FETI-2LM.

3.3. Incorporation of the second-level coarse problem

The incorporation in the FETI-2LM method of the second-level coarse problem presented in Sections 2.5 and 2.6 follows the same principles as those described in Section 2.5 and Remark 1. However, because the interface problem matrix $\mathbf{f}_I$ associated with the FETI-2LM method is complex and unsymmetric, the $\mathbf{A}$-norm to be considered in Remark 1 is the $\mathbf{F}_I^*\mathbf{F}_I$-norm. This implies that constraint (20) should be replaced by

$$\mathbf{Q}^*\mathbf{F}_I^*\mathbf{r}^k = \mathbf{Q}^*\mathbf{F}_I^*(\mathbf{d} - \mathbf{F}_I\boldsymbol{\lambda}) = 0. \tag{48}$$

Again, a straightforward approach for enforcing Eq. (48) at each ORTHODIR iteration is to transform each iterate $\boldsymbol{\lambda}^k$ into $\widetilde{\boldsymbol{\lambda}}^k$ as specified in Eq. (22). Substituting Eq. (22) into Eq. (48) gives

$$\widetilde{\boldsymbol{\lambda}}^k = \mathbf{P}\boldsymbol{\lambda} + \boldsymbol{\lambda}^0,$$

where

$$\begin{aligned}\mathbf{P} &= \mathbf{I} - \mathbf{Q}[(\mathbf{F}_I\mathbf{Q})^*(\mathbf{F}_\mathbf{I}\mathbf{Q})]^{-\mathbf{1}}(\mathbf{F}_\mathbf{I}\mathbf{Q})^*\mathbf{F}_\mathbf{I},\\ \boldsymbol{\lambda}^\mathbf{0} &= \mathbf{Q}[(\mathbf{F}_\mathbf{I}\mathbf{Q})^*(\mathbf{F}_\mathbf{I}\mathbf{Q})]^{-\mathbf{1}}(\mathbf{F}_\mathbf{I}\mathbf{Q})^*\mathbf{d}.\end{aligned} \tag{49}$$

In the sequel, we refer to the regularized FETI-2LM method preconditioned by the projector **P** specified in Eq. (49) as the FETI-H-2LM method. This method is summarized in Box 2 where the parentheses around a quantity have the same meaning as in Box 1.

Box 2. The two-level FETI-H method for exterior Helmholtz problems

1. Initialize

$$\begin{aligned}\boldsymbol{\lambda}^0 &= \mathbf{Q}[[\mathbf{F}_I\mathbf{Q}]^*[\mathbf{F}_I\mathbf{Q}]]^{-1}(\mathbf{F}_I\mathbf{Q})^*\mathbf{d},\\ \mathbf{r}^0 &= \mathbf{d} - \mathbf{F}_I\boldsymbol{\lambda}^0,\\ \mathbf{p}^0 &= \mathbf{P}\mathbf{r}^0,\\ (\mathbf{F}_I\mathbf{p})^0 &= \mathbf{F}_I\mathbf{p}^0,\end{aligned}$$

2. Iterate $k = 1, 2, \ldots$ until convergence

$$\begin{aligned}\rho^k &= (\mathbf{F}_I\mathbf{p})^{k-1^*}\mathbf{r}^{k-1}/(\mathbf{F}_I\mathbf{p})^{k-1^*}(\mathbf{F}_I\mathbf{p})^{k-1},\\ \boldsymbol{\lambda}^k &= \boldsymbol{\lambda}^{k-1} - \rho^k\mathbf{p}^{k-1},\\ \mathbf{r}^k &= \mathbf{r}^{k-1} - \rho^k(\mathbf{F}_I\mathbf{p})^{k-1},\\ \zeta^l &= -(\mathbf{F}_I\mathbf{p})^{l^*}\mathbf{F}_I\mathbf{P}(\mathbf{F}_I\mathbf{p})^{k-1}/(\mathbf{F}_I\mathbf{p})^{l^*}(\mathbf{F}_I\mathbf{p})^l, \quad 0 \leqslant l \leqslant k-1,\\ \mathbf{p}^k &= \mathbf{p}(\mathbf{F}_I\mathbf{p})^{k-1} + \sum_{l=0}^{k-1}\zeta^l\mathbf{p}^l,\\ (\mathbf{F}_I\mathbf{p})^k &= \mathbf{F}_I\mathbf{P}(\mathbf{F}_I\mathbf{p})^{k-1} + \sum_{l=0}^{k-1}\zeta^l(\mathbf{F}_I\mathbf{p})^l.\end{aligned} \tag{50}$$

Like the FETI-H method, the FETI-H-2LM method requires only one projection of the form **Ps** and one matrix–vector product of the form $\mathbf{F}_I\mathbf{t}$ per iteration, where **s** and **t** are two generic interface vectors. The parallelization of FETI-H-2LM is similar to that of the FETI-H method.

Finally, we point out that the residual associated with the FETI-H-2LM method does not correspond to the jump of the solution across the subdomain interfaces, but to the jump of the radiation condition across these interfaces. Hence, if $\mathbf{Q}^s_{\mathrm{pw}}$ is the subdomain prolongation of the subdomain interface matrix of planar waves introduced in Section 2.6, an appropriate subdomain matrix $\mathbf{Q}^s$ for generating the second-level coarse problem of the FETI-H-2LM method is

$$\mathbf{Q}^s = \mathbf{B}^s[\widetilde{\mathbf{K}}^s + \mathrm{i}k\mathbf{B}^s_T]\mathbf{Q}^s_{\mathrm{pw}}\mathbf{Q}^s_{\mathrm{pw}}, \tag{51}$$

where $\mathbf{M}^s_I = \sum_{\Gamma^m_I \subset \Omega^s}\mathbf{B}^{s^{\mathrm{T}}}_{\Gamma^m_I}\left[\mathbf{M}^{\Gamma^m_I}_{bb}\right]\mathbf{B}^s_{\Gamma^m_I}$.

3.4. Convergence properties of the regularized FETI-2LM method

In order to investigate numerically the convergence properties of the regularized FETI-2LM method, we consider again the guided wave problem depicted in Fig. 4 and discussed in Sections 2.7 and 2.8. First, we set the wavenumber to $ka = 20$ and consider again the four meshes corresponding to $h = 1/100$, $h = 1/150$, $h = 1/200$ and $h = 1/250$, and for each of these meshes a 5×5 mesh partition. We apply the regularized FETI-2LM method to the solution of the resulting systems of equations, and monitor its convergence using the same criterion as in (32). We report in Table 6 the obtained performance results along with those previously tabulated for the regularized FETI method with one Lagrange multiplier field. These results

Table 6
The guided wave problem – $ka = 20$ – $N_s = 25$ (regularized FETI vs. regularized FETI-2LM)

h	Number of iterations (FETI)	Number of iterations (FETI-2LM)
1/100	91	139
1/150	94	144
1/200	96	143
1/250	96	143

Table 7
The guided wave problem – $ka = 20$ – $h = 1/200$ (regularized FETI vs. regularized FETI-2LM)

N_s	Number of iterations (FETI)	Number of iterations (FETI-2LM)
4	31	59
16	71	118
25	96	143

Table 8
The guided wave problem – $h = 1/315$ – $N_s = 25$ (regularized FETI can be vs. regularized FETI-2LM)

ka	Number of iterations (FETI)	Number of iterations (FETI-2LM)
20	97	144
40	136	168
60	167	235

show that the regularized FETI-2LM method is also scalable with respect to the mesh size h; however, it is outperformed by the regularized FETI method with one Lagrange multiplier field.

As in Section 2.7, we focus next on the case $h = 1/200$ with 2×2, 4×4 and 5×5 mesh partitions. From the results reported in Table 7, we de that, like the regularized FETI method with one Lagrange multiplier field, the unpreconditioned regularized FETI-2LM method does not scale with the number of subdomains.

Finally, we fix the mesh size to $h = 1/315$, partition Ω into 5×5 subdomains, and consider three different wavenumbers corresponding to $ka = 20$, $ka = 40$, and $ka = 60$. The performance results we report in Table 8 demonstrate that in the absence of a preconditioner, the number of iterations for convergence of the regularized FETI-2LM method also increases sublinearly with the wavenumber.

In summary, the convergence properties of the unpreconditioned regularized FETI methods with a single and two Lagrange multiplier fields are similar. Without preconditioning, both methods are scalable with respect to mesh size h, but not with respect to the subdomain size H and the wavenumber k. However, at least for the guided wave problem considered here, the FETI method with a single Lagrange multiplier field outperforms its two-field variant for any given mesh, mesh partition, and wavenumber.

Next, we investigate the convergence properties of the regularized FETI method with two Lagrange multiplier fields when equipped with the preconditioner described in Section 3.3. We use for this purpose the same guided wave problem as in this section.

3.5. Convergence properties of the FETI-H-2LM method

As in Section 2.8, we consider three different scattering problems corresponding to $ka = 20$, $ka = 40$ and $ka = 60$. We fix the mesh size to $h = 1/315$, and vary the number of subdomains between 4 and 16. For each case, we consider three different coarse problems with N_θ equal to 4, 8, and 16, respectively. We report in Table 9 the performance results obtained using the FETI-H-2LM method and contrast them with those of the FETI-H method. These results show that, as the FETI-H method, the FETI-H-2LM method is also

Table 9
The guided wave problem – $h = 1/315$ (regularized FETI vs. regularized FETI-2LM)

ka	N_0	N_s	Size of the coarse problem	Size of the problem	Number of problem	Number of iterations
20	8	4	20	36	19	62
20	8	9	54	81	20	85
20	8	16	105	144	20	83
20	16	4	30	68	18	43
20	16	9	71	130	19	52
20	16	16	129	225	17	55
20	32	4	30	67	19	38
20	32	9	80	149	20	50
20	32	16	126	249	18	54
40	8	4	20	36	24	67
40	8	9	56	81	30	101
40	8	16	108	144	36	119
40	16	4	38	64	19	56
40	16	9	84	147	23	71
40	16	16	169	260	17	57
40	32	4	48	92	18	39
40	32	9	83	217	18	42
40	32	16	175	365	18	42
60	8	4	20	36	31	86
60	8	9	56	81	59	134
60	8	16	108	144	55	180
60	16	4	40	64	18	76
60	16	9	197	149	21	113
60	16	16	203	266	19	143
60	32	4	61	108	15	46
60	32	9	138	245	16	51
60	32	16	233	434	31	58

scalable with respect to the number of subdomains. However, these results also highlight the superiority of the FETI-H method over its two-field variant.

4. The FETI-H method vs. its two-field variant

The FETI-H and FETI-H-2LM methods share the same basic ideas and principles but differ in the implementation of these principles. The FETI-H method is based on a classical hybrid domain decomposition formulation and is characterized by a symmetric interface problem matrix. The FETI-H-2LM method is based on a three-field domain decomposition formulation and leads to an unsymmetric interface problem matrix. Consequently, each method employs a similar but yet different Krylov based iterative scheme for solving its interface problem, and a similar but yet different coarse problem based preconditioner for accelerating convergence. So far, the performance results summarized in Tables 1–9 suggest that the FETI-H method has superior convergence properties, and that the second-level coarse problem constructed with planar waves is more effective for the FETI-H method than for its three-field counterpart.

However, a fair comparison of the FETI-H and FETI-H-2LM methods calls for the additional comparison of CPU solution timings, as the FETI-H-2LM does offer some computational advantages in the construction of the second-level problem matrix. For example, consider a two-dimensional uniform mesh partitioned in a checkerboard fashion. When forming the matrix product $\mathbf{F}_I\mathbf{Q}$, for each planar wave and in each subdomain Ω^s, the FETI-H method performs 9 subdomain computations of the form $\mathbf{F}_I^s\mathbf{Q}^q$ where $\mathbf{F}_I^s = \mathbf{B}^s(\widetilde{\mathbf{K}}^s + \mathrm{i}k\mathbf{M}_I^s)^{-1}\mathbf{B}^{s^{\mathrm{T}}}$, and the superscript q designates Ω^s itself and its 8 neighboring subdomains. On the other hand, when forming the same product $\mathbf{F}_I\mathbf{Q}$, for each planar wave and in each subdomain Ω^s, the

Table 10
The guided wave problem – $h = 1/240$ (FETI-H vs. FETI-H-2LM performance results on a 16-processor Origin 2000)

ka	N_θ	N_s	Number of iterations (FETI-H)	Number of iterations (FETI-H-2LM)	Total CPU time (FETI-H-2LM) (s)	Total CPU time (FETI-H-2LM) (s)
20	8	16	16	83	4.7	8.8
20	16	16	15	55	6.3	9.3
20	32	16	15	54	10.9	22.9
40	8	16	23	119	5.3	12.3
40	16	16	14	57	6.3	9.5
40	32	16	15	42	10.7	20.8
60	8	16	51	180	8.1	18.8
60	16	16	14	143	6.3	22.3
60	32	16	13	58	10.8	28.1

FETI-H-2LM method performs a single computation of the form $\mathbf{F}_I^s\mathbf{Q}^q$ because two Lagrange multiplier fields are used on the interface boundary of Ω^s. This could have been a significant computational advantage for the FETI-H-2LM method, except that:

- the computational cost of forming $\mathbf{F}_I\mathbf{Q}$ increases linearly with the number of planar wave directions N_θ;
- the computational cost of constructing the complete second-level problem matrices $\mathbf{Q}^T\mathbf{F}_I\mathbf{Q}$ and $(\mathbf{F}_I\mathbf{Q})^*(\mathbf{F}_I\mathbf{Q})$ grows quadratically with the number of planar wave directions N_θ, and that cost is similar for both the FETI-H and FETI-H-2LM methods.

Hence, the computational overhead associated with forming the second-level coarse problem should be smaller for the FETI-H-2LM method when N_θ is relatively small, and comparable for both FETI-H and FETI-H-2LM methods when N_θ becomes more significant.

Here, we consider again the guided wave problem depicted in Fig. 4. We fix the mesh size to $h = 1/240$, and the number of subdomains to $N_s = 16$. We vary the wavenumber between $ka = 20$ and $ka = 60$, and for each case we vary N_θ between 8 and 32. We apply both the FETI-H and FETI-H-2LM methods to the solution of this problem, and report in Table 10 the performance results obtained on a 16-processor Origin 2000 computer. Before commenting on these performance results, we note that:

- each of the two FETI methods has been programmed by different investigators using a different programming language: C++ for the FETI-H method, and FORTRAN 90 for the FETI-H-2LM method;
- the FETI-H method has been implemented for arbitrary mesh configurations and mesh partitions. The FETI-H-2LM code has been optimized for checkerboard mesh partitions. In particular, it does not employ any Lagrange multiplier for assembling two subdomains that intersect only at a crosspoint [10];
- otherwise, both methods employ the same stopping criterion (32), and both corresponding codes share similar parallelization paradigms.

The performance results reported in Table 10 show that the FETI-H method performs anywhere between 3 and 10 times less iterations than the FETI-H-2LM method, and is 2 to 4 times faster CPU-wise. The discrepancy between the differences for these two FETI methods in iteration count and CPU time is explained by the computational overhead associated with the second-level coarse problem which, when convergence is fast, becomes a significant portion of the total CPU solution time, as illustrated next. In any case, the performance results displayed in Table 10 illustrate the computational efficiency of the FETI-H method, and demonstrate its superiority over the FETI-H-2LM variant.

5. Parallel acoustic scattering computations using the FETI-H method

Here, we consider the two-dimensional solution of two sound-soft acoustic scattering problems where the obstacle has the shape of a submarine (Fig. 5) of length L. The first problem is characterized by $kL = 50$, and the second one by $kL = 100$. In the first case, we discretize the exterior domain by 314265 $P1$ elements and 157801 grid points, and partition the corresponding mesh into 16, 32, and 64 subdomains using the

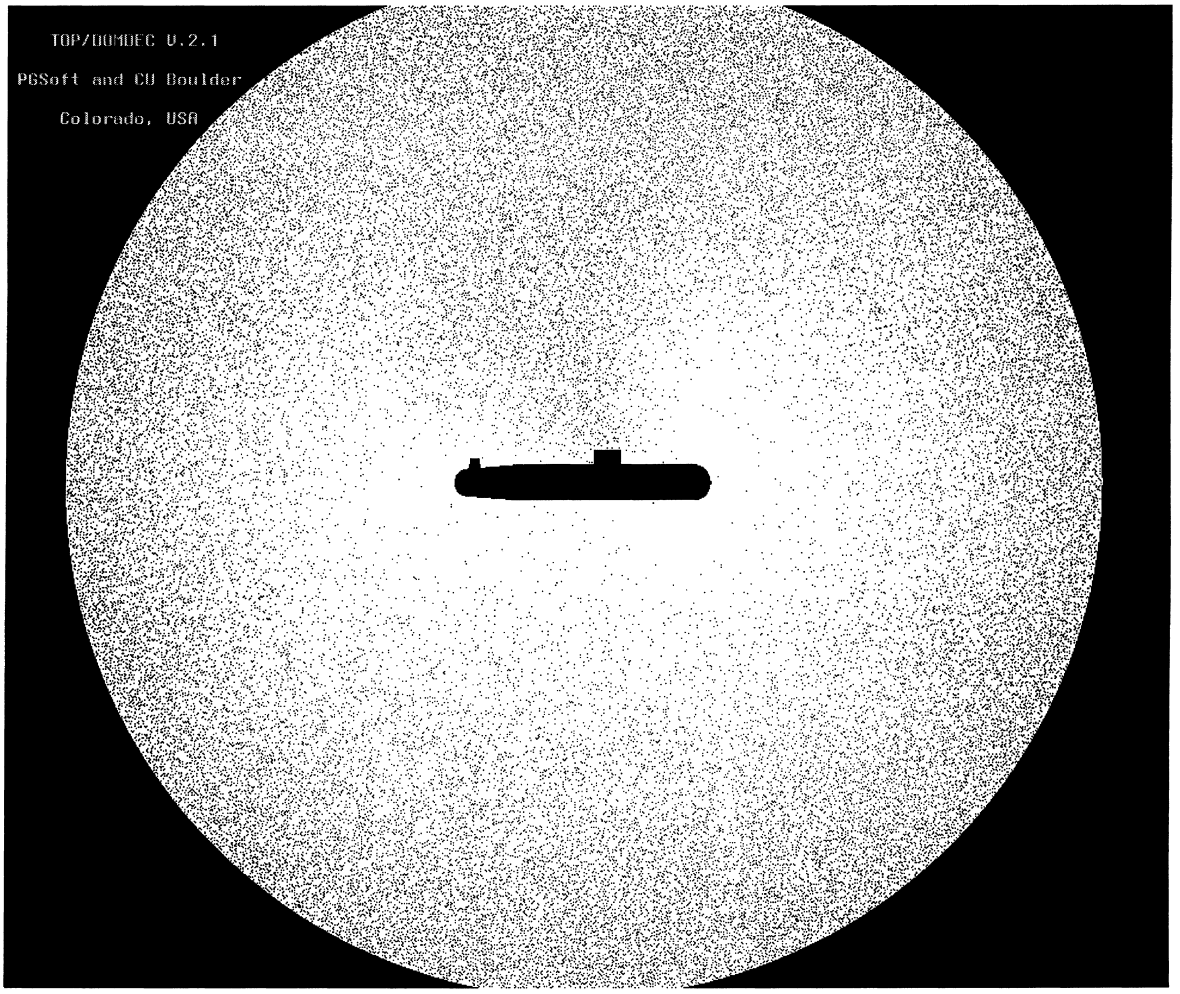

Fig. 5. Discretization of the surrounding of a submarine.

TOP/DOMDEC software package (Fig. 6) [26]. In the second case, we discretize the computational domain by 1075264 $Q1$ elements and 1077432 nodes, and decompose the corresponding mesh into 50, 100, and 200 subdomains. The change from $P1$ to $Q1$ elements is only for the purpose of illustrating our DD methodology for different finite element discretizations. For both problems, we employ only the FETI-H method for solving the resulting systems of equations, because we have already shown that this method is superior to its two-field variant. We perform all computations on an Origin 2000 parallel processor, and monitor convergence using the same criterion as in (32).

For the first problem, the solution of the resulting system of equations by a direct skyline solver requires 2343.4 s on a single processor of our Origin 2000. This performance is not tainted by memory swapping as the memory available on our machine is large enough to meet the requirements of the direct skyline solver for this problem. The performance of the FETI-H method applied to the solution of this same problem on a single Origin 2000 processor is summarized in Table 11.

The performance results displayed in Table 11 confirm again the numerical scalability of the FETI-H method with respect to the number of subdomains, and the relative importance for convergence of N_θ and the sheer size of the coarse problem. The reader can observe that the cost of forming the second-level FETI problem can be a significant percentage of the total solution cost. For a fixed N_θ, the cost of forming $\mathbf{Q}^{\mathrm{T}}\mathbf{F}_I\mathbf{Q}$ is affected by N_s in two different ways. For a fixed mesh size h, increasing the number of subdomains decreases the size of the subdomain problems and therefore has a tendency to reduce the CPU time needed for forming $\mathbf{Q}^{\mathrm{T}}\mathbf{F}_I\mathbf{Q}$. However, increasing the number of subdomains also increases both the number of col-

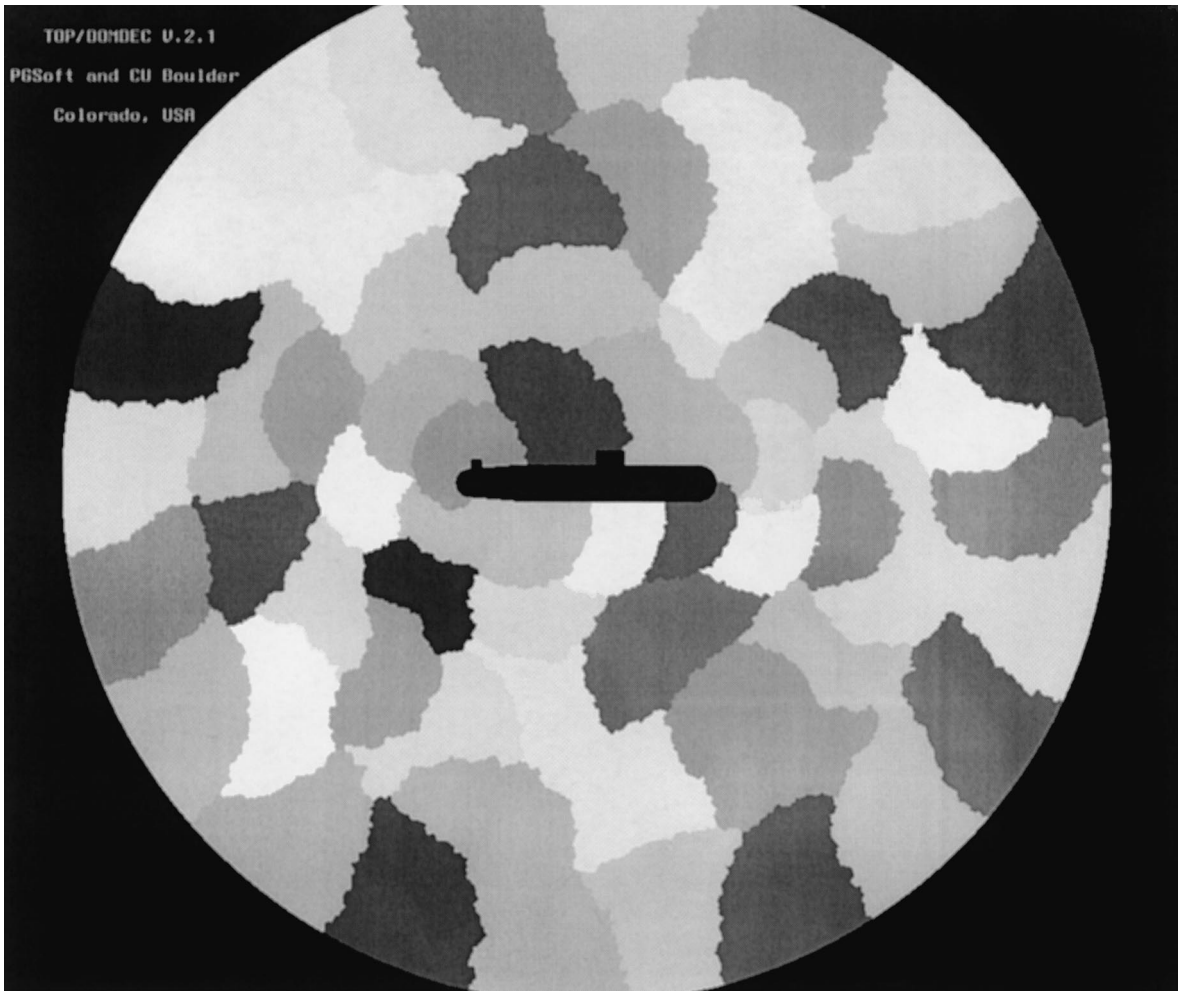

Fig. 6. Mesh partitioning.

Table 11
The submarine problem – $kL = 50$ – 157 801 unknowns (performance results of the FETI-H method on one Origin 2000 processor)

N_0	N_s	Size of the coarse problem	Number of iterations	CPU time for forming $\mathbf{Q}^T\mathbf{F}_I\mathbf{Q}$ (s)	Total CPU time (s)
20	16	300	187	179.7	854.2
20	32	620	87	145.0	393.6
20	64	1244	88	104.7	250.5
24	16	360	94	216.1	578.4
24	32	744	65	174.2	368.5
24	64	1512	49	125.4	242.0
32	16	480	50	288.5	504.4
32	32	988	46	233.2	392.8
32	64	1996	30	171.0	263.5

umns in $\mathbf{Q}$ and the number of subdomain problems to be solved, and therefore has also a tendency to increase the CPU time required for forming the second-level problem matrix. For the first submarine problem discussed here, the first of these two effects prevails as it is shown in Table 11 that for all three

values of N_θ, the cost of forming $\mathbf{Q}^T\mathbf{F}_I\mathbf{Q}$ decreases when N_s is increased. Furthermore, the reader can observe in Table 11 that for a given N_θ, the total CPU time decreases when the number of subdomains is increased. Again, this is because when the problem size is fixed and the number of subdomains is increased, the size of the local problems is decreased, and therefore the CPU time associated with factoring the local matrixes and performing all local forward and backward substitutions also decreases. In all cases, the FETI-H method is shown to outperform the direct solver. In the best case ($N_\theta = 24$, $N_s = 64$), the FETI-H method solves the first submarine problem in seconds and therefore outperforms the direct method by a factor that is almost equal to a full-order of magnitude. Note that this performance is better than that reported in [8] for the same submarine problem, because here FETI-H is equipped with GCR, whereas in [8] it was equipped with CR. For the best case ($N_\theta = 24$, $N_s = 64$), the parallel performance results of the FETI-H method are reported in Table 12. Note that in this work, we employ the parallel skyline solver presented in [27] for solving in parallel all coarse problems. Good speedups are obtained up to processors For a number of processors larger than, an average to a small speedup is achieved in all phases of the FETI-

Table 12
The submarine problem – $kL = 50$ – 157801 unknowns (parallel performance results of the FETI-H method on a 24-processor Origin 2000 $N_\theta = 24$, $N_s = 64$)

Number of processors	CPU time for forming $\mathbf{Q}^T\mathbf{F}_I\mathbf{Q}$ (s)	CPU time for factoring $\mathbf{Q}^T\mathbf{F}_I\mathbf{Q}$ (s)	Total FETI-H CPU time (s)	Parallel efficiency (%)
1	125.4	3.4	242.0	–
2	63.3	2.0	128.8	93.9
4	37.0	1.3	80.7	74.9
8	20.2	1.0	45.7	66.2
12	15.5	1.0	36.9	54.6
16	10.7	1.1	28.2	53.6
20	10.0	1.1	28.9	41.8
24	8.5	1.2	27.1	37.2

Table 13
The submarine problem – $kL = 100$ – 1077432 unknowns (performance results of the FETI-H method on 24 Origin 2000 processors)

N_θ	N_s	Number of iterations	CPU time for forming $\mathbf{Q}^T\mathbf{F}_I\mathbf{Q}$ (s)	Total CPU time (s)
32	50	44	171.6	304.1
32	100	40	126.2	239.1
32	200	51	92.1	216.0

Table 14
The submarine problem – $kL = 100$ – 1077432 unknowns (parallel performance results of the FETI-H method on a 24-processor Origin 2000 $N_\theta = 32$, $N_s = 200$)

Number of processors	CPU time for forming $\mathbf{Q}^T\mathbf{F}_I\mathbf{Q}$ (s)	CPU time for factoring $\mathbf{Q}^T\mathbf{F}_I\mathbf{Q}$ (s)	Total FETI-H CPU time (s)	Parallel efficiency (%)
1	1950.9	114.7	3418.4	–
2	929.7	53.1	1646.0	103.5
4	508.7	26.9	966.1	88.4
8	239.2	17.3	474.5	90.1
12	177.0	14.0	370.2	76.9
16	135.4	13.2	302.7	70.6
20	117.3	13.2	274.0	62.4
24	92.1	13.1	216.0	65.9

H method, which can be expected for such a relatively small size problem. Note that our parallel implementation of the FETI-H method is not limited to assigning one subdomain to one processor. (The results reported inTable 12 are for subdomains and a number of processors varying between 1 and 24.)

For the second submarine problem, we set $N_\theta = 32$ and partition the mesh into 50, 100, and 200 subdomains.

The performance results of the FETI-H method applied to the solution of the second submarine problem on a 24-processor Origin 2000 are reported in Table 13. These results exhibit the same trends as those reported in Table 11 for the first submarine problem. For the 200-subdomain case, Table 14 shows that good speedups are achieved up to 24 processors, which demonstrates the parallel scalability of our implementation of the FETI-H method on the Origin 2000.

6. Conclusions

In this paper, we have presented two two-level domain decomposition (DD) methods for solving iteratively large-scale systems of equations arising from the finite element discretization of high-frequency exterior Helmholtz problems. Both methods are FETI methods for indefinite or complex problems. They distinguish themselves from previous FETI algorithms in the elimination of local resonance via the stabilization of each subdomain problem matrix by a complex interface mass matrix. The first DD method employs one Lagrange multiplier field to glue the subdomain solutions at the subdomain interfaces. It leads to a symmetric but not Hermitian interface problem that is most efficiently solved by the generalized conjugate residual method. The second DD method is a three-field variant that employs two Lagrange multiplier fields at the subdomain interfaces. It leads to an unsymmetric interface problem that is solved by the ORTHODIR algorithm. A unique characteristic of both DD methods is that, even in the absence of any preconditioner, they are scalable with respect to the mesh size. When equipped with a second-level FETI coarse problem based on planar waves and which plays the role of a global preconditioner, they become also scalable with respect to both the subdomain size and the wavenumber. However, this coarse problem appears to be more effective for the first FETI based DD method than for its three-field variant. Sample CPU timings for realistic two-dimensional acoustic scattering problems highlight a great potential, at least for the first proposed DD method, for the *fast* and *scalable* solution of three-dimensional high-frequency exterior Helmholtz problems.

Acknowledgements

The US authors acknowledge the support by the Office of Naval Research under Grant N-00014-95-1-0663. The second author also acknowledges the financial support by a Brazilian CAPES Fellowship, Process No. 1233/95-2.

Appendix A

Let Γ^s denote the (interface) boundary of a subdomain Ω^s, and Γ^s_b the subset of Γ^s on which the regularization matrix $\mathbf{M}^s_I$ introduced in this paper is defined. By construction, Γ^s_b has a non-zero measure. Given a subdomain vector $\mathbf{u}^s$, we partition it as

$$\mathbf{u}^s = \begin{bmatrix} \mathbf{u}^s_r \\ \mathbf{u}^s_b \end{bmatrix}, \tag{A.1}$$

where the subscript b designates the unknowns associated with Γ^s_b, and the subscript r designates the remainder of $\mathbf{u}^s$. By construction, if Ω^s belongs to a checkerboard mesh decomposition then $\Gamma^s_b = \Gamma$, and if Ω^s belongs to an arbitrary mesh decomposition then $\Gamma^s_b \subset \Gamma$. In both cases, the regularizing matrix $\mathbf{M}^s_I$ proposed in this paper can be written as

$$\mathbf{M}_I^s = \begin{bmatrix} 0 & 0 \\ 0 & \mathbf{M}_{bb}^s \end{bmatrix}, \tag{A.2}$$

where $\mathbf{M}_{bb}^s$ has a constant sign along Γ_b^s, and therefore $\mathbf{M}_{bb}^s$ is either symmetric positive definite or symmetric negative definite. Given a symmetric positive semi-definite subdomain stiffness matrix $\mathbf{K}^s$, a symmetric positive definite mass matrix $\mathbf{M}^s$, and a wavenumber k, the following holds.

Theorem A.1. *For any given positive real number ω^2 and the regularizing matrix $\mathbf{M}_I^s$ proposed in this paper and summarized above, the complex matrix $\mathbf{K}^s - \omega^2\mathbf{M}^s + \mathrm{i}k\mathbf{M}_I^s$ is invertible.*

Proof. Suppose there exists a vector

$$\mathbf{u}^s = \begin{bmatrix} \mathbf{u}_r^s \\ \mathbf{u}_b^s \end{bmatrix}$$

satisfying

$$(\mathbf{K}^s - \omega^2\mathbf{M}^s + \mathrm{i}k\mathbf{M}_I^s)\mathbf{u}^s = 0. \tag{A.3}$$

Premultiplying the above equation by $\mathbf{u}_s^*$, where the $*$ superscript denotes the transpose of the complex conjugate of a quantity, leads to

$$\mathbf{u}^{s^*}(\mathbf{K}^s - \omega^2\mathbf{M}^s)\mathbf{u}^s = -\mathrm{i}k\mathbf{u}^{s^*}\mathbf{M}_I^s\mathbf{u}^s. \tag{A.4}$$

Since $(\mathbf{K}^s - \omega^2\mathbf{M}^s)$ and $\mathbf{M}_I^s$ are two real symmetric matrices, it follows that the left-hand side of Eq. (A.4) is a real number, and the right-hand side of that equation is an imaginary number, which implies that

$$\mathbf{u}^{s^*}(\mathbf{K}^s - \omega^2\mathbf{M}^s)\mathbf{u}^{s^*} = 0 \tag{A.5}$$

and

$$\mathbf{u}^{s^*}\mathbf{M}_I^s\mathbf{u}^s = 0. \tag{A.6}$$

If ω^2 is not an eigenvalue of the pencil $(\mathbf{K}^s, \mathbf{M}^s)$, then Eq. (A.4) implies $\mathbf{u}^s = 0$, which concludes the proof of Theorem A.1.

On the other hand, if ω^2 is an eigenvalue of the pencil $(\mathbf{K}^s, \mathbf{M}^s)$, then from Eqs. (A.2)–(A.4) it follows that

$$\mathbf{u}_b^s = 0 \tag{A.7}$$

which transforms Eq. (A.5) into

$$\mathbf{u}_r^{s^*}(\mathbf{K}_{rr}^s - \omega^2\mathbf{M}_{rr}^s)\mathbf{u}_r^s = 0. \tag{A.8}$$

Here again, two cases can be distinguished. If ω^2 is not an eigenvalue of the pencil $(\mathbf{K}_{\mathbf{rr}}^{\mathbf{s}}, \mathbf{M}_{\mathbf{rr}}^{\mathbf{s}})$, then Eq. (A.8) implies

$$\mathbf{u}_r^s = 0. \tag{A.9}$$

From Eqs. (A.7) and (A.8), if follows that $\mathbf{u}^s = 0$, which concludes the proof of Theorem A.1. If ω^2 is an eigenvalue of the pencil $(\mathbf{K}_{rr}^s, \mathbf{M}_{rr}^s)$, then from Eq. (A.3) it follows that $\mathbf{u}^s$ is the discrete solution of an elliptic problem with homogeneous Neumann boundary conditions, and from Eq. (A.8) it follows that $\mathbf{u}^s$ is also the discrete solution of the same elliptic problem but with homogeneous Dirichlet boundary conditions. This in turn implies that $\mathbf{u}^s$ is a continuous discretization of a function that vanishes simultaneously with its normal derivative on a boundary Γ_b^s with a non-zero measure. From Holmgren's continuation theorem [28], it follows that $\mathbf{u}^s = 0$, which concludes the proof of Theorem A.1.

References

[1] B. Després, Décomposition de domaine et problème de helmholtz, Compte Rendu de l'Académie des Sciences, France, 311 (Série I) (1990) 313–316.
[2] B. Lee, T. Manteuffel, S. McCormick, J. Ruge, Multilevel first-order system least squares for Helmholtz equation, Proceedings of second International Conference on Approximation and Numerical Methods for the Solution of the Maxwell Equations, Wiley, Washington, DC, 1993.
[3] J. Benamou, B. Després, A domain decomposition method for the Helmholtz equation and related optimal control problems, Rapport de recherche INRIA No. 2791, 1996.
[4] M. Malhotra, R. Freund, P.M. Pinsky, Iterative solution of multiple radiation and scattering problems in structural acoustics using a block quasi-minimal residual algorithm, Comput. Meth. Appl. Mech. Eng. 146 (1997) 173–196.
[5] A. LaBourdonnaye, C. Farhat, A. Macedo, F. Magoulès, F.X. Roux, A non-overlapping domain decomposition method for the exterior Helmholtz problem, Contemporary Mathematics 218 (1998) 42–66.
[6] P. Vanvek, J. Mandel, Marian Brezina, Two-level algebraic multigrid for the Helmholtz problem, Contemporary Mathematics 218 (1998) 349–356.
[7] X.-C. Cai, M.A. Casarin Jr., F.W. Elliott Jr., O.B. Widlund, Overlapping Schwarz algorithms for solving Helmholtz's equation, Contemporary Mathematics 218 (1998) 390–398.
[8] C. Farhat, A. Macedo, M. Lesoinne, A two-level domain decomposition method for the iterative solution of high frequency exterior Helmholtz problems, Numerische Mathematik, submitted for publication.
[9] C. Farhat, P.S. Chen, F.X. Roux, The dual schur complement method with well-posed local Neumann problems: regularization with a perturbed lagrangian formulation, SIAM J. Sci. Stat. Comput. 14 (1993) 752–759.
[10] C. Farhat, F.X. Roux, An unconventional domain decomposition method for an efficient parallel solution of large-scale finite element systems, SIAM J. Sci. Stat. Comput. 13 (1992) 379–396.
[11] C. Farhat, J. Mandel, F.X. Roux, Optimal convergence properties of the FETI domain decomposition method, Comput. Meth. Appl. Mech. Eng. 115 (1994) 367–388.
[12] J. Mandel, R. Tezaur, Convergence of a substructuring method with Lagrange multipliers, Numerische Mathematik 73 (1996) 473–487.
[13] C. Farhat, J. Mandel, The two-level FETI method for static and dynamic plate problems – Part I: an optimal iterative solver for biharmonic systems, Comput. Meth. Appl. Mech. Eng. 155 (1998) 129–152.
[14] C. Farhat, M. Géradin, On the general solution by a direct method of a large-scale singular system of linear equations: application to the analysis of floating structures, Internat. J. Numer. Meth. Eng. 41 (1998) 675–696.
[15] L. Franca, C. Farhat, M. Lesoinne, A. Russo, Unusual stabilized finite element methods and residual-free bubbles, Internat. J. Numer. Meth. in Fluids 27 (1998) 159–168.
[16] L. Franca, C. Farhat, A. Macedo, M. Lesoinne, Residual-free bubbles for the Helmholtz equation, Internat. J. Numer. Meth. Eng. 40 (1997) 4003–4009.
[17] J.L. Lions, R. Dautray, Analyse mathématique et calcul numérique pour les sciences et techniques, Tome 1, Masson, Paris, 1985.
[18] Y. Saad, Iterative Methods for Sparse Linear Systems, PWS Publishing Company, Boston, 1995.
[19] A. Macedo, On the choice of a Krylov method for a domain decomposed iterative solution of the exterior Helmholtz problem, Eleventh International Conference on Domain Decomposition Methods, London, England, 20–24 July 1998.
[20] B.D. Craven, Complex symmetric matrices, J. Austral. Math. Soc 10 (1969) 341–354.
[21] C. Farhat, P.S. Chen, J. Mandel, A scalable Lagrange multiplier based domain decomposition method for implicit time-dependent problems, Internat. J. Numer. Meth. Eng. 38 (1995) 3831–3854.
[22] C. Farhat, P.S. Chen, F. Risler, F.X. Roux, A unified framework for accelerating the convergence of iterative substructuring methods with lagrange multipliers, Internat. J. Numer. Meth. Eng. 42 (1998) 257–288.
[23] S.F. Ashby, T.A. Manteuffel, P.E. Saylor, A taxonomy for conjugate gradient methods, SIAM J. Numer. Anal. 27 (1990) 1542–1568.
[24] C. Farhat, M. Lesoinne, K. Pierson, The second generation FETI methods and their application to the parallel solution of large-scale linear and geometrically nonlinear structural analysis problems, Comput. Meths. Appl. Mech. Eng. 184 (2000) 333–374.
[25] F. Brezzi, L.D. Marini, A three-field domain decomposition method, Contemporary Mathematics 157 (1993) 27–34.
[26] C. Farhat, S. Lantéri, H.D. Simon, TOP/DOMDEC a software tool for mesh partitioning and parallel processing, J. Comput. Sys. Eng. 6 (1995) 13–26.
[27] C. Farhat, Redesigning the skyline solver for parallel/vector supercomputers, Internat. J. High Speed Comput. 2 (1990) 223–238.
[28] L. Hormander, Linear Partial Differential Operators, Springer, Berlin, 1963.